ELSEVIER

Carbohydrate Research 285 (1996) 99–128

CARBOHYDRATE RESEARCH

The structures of arabinoxyloglucans produced by solanaceous plants [1]

William S. York *, V.S. Kumar Kolli, Ron Orlando, Peter Albersheim, Alan G. Darvill

Complex Carbohydrate Research Center and Department of Biochemistry and Molecular Biology, University of Georgia, 220 Riverbend Road, Athens, GA 30602-4712, USA

Received 29 September 1995; accepted 9 January 1996

Abstract

Several structural features, most notably the presence of α-L-Ara*f*-(1 → 2)-α-D-Xyl*p* side chains, distinguish the arabinoxyloglucans (AXGs) produced by solanaceous plants from the xyloglucans produced by other dicotyledonous plants. However, previous studies did not establish the exact order of attachment of the various side chains along the backbone of these AXGs. Therefore, oligosaccharide subunits of the AXGs secreted by suspension-cultured tobacco and tomato cells were generated by treatment of the isolated AXGs with a fungal *endo*-β-(1 → 4)-D-glucanase (EG). The oligosaccharides were reduced with sodium borohydride to the corresponding oligoglycosyl alditol derivatives and purified by a combination of gel-permeation chromatography, reversed-phase HPLC, and HPAE chromatography. The isolated oligoglycosyl alditols were chemically characterized by NMR spectroscopy, matrix-assisted laser-desorption/ionization time-of-flight mass spectrometry (MALDITOFMS), fast-atom bombardment mass spectrometry (FABMS), FABMS/MS, and glycosyl-linkage analysis. The results confirmed that the AXGs from these species are composed of a (1 → 4)-linked β-D-Glc*p* backbone substituted at O-6 with various side chains. Both tobacco and tomato AXG contain α-D-Xyl*p* and α-L-Ara*f*-(1 → 2)-α-D-Xyl*p* side chains. However, oligosaccharide fragments of tomato AXG were also shown to contain β-D-Gal*p*-(1 → 2)-α-D-Xyl*p* and β-Ara*f*-(1 → 3)-α-L-Ara*f*-(1 → 2)-α-D-Xyl*p* side chains that are not present in the tobacco AXG. This is the first report of β-Ara*f* residues in a xyloglucan. The primary structures of 20 oligosaccharides generated by EG-treatment of tobacco AXG were determined. The generation of such a large number of oligosaccharides is due in part to the presence of *O*-acetyl substituents at O-6 of many of the backbone β-D-Glc*p* residues of tobacco AXG. The presence of either an *O*-acetyl or a glycosidic substituent at O-6 of a β-D-Glc*p*

* Corresponding author. Fax: + 1-706-542-4412.

[1] This article is number XLII in the series entitled, "The Structure of Plant Cell Walls."

PII S0008-6215(96)00029-8

residue in the AXG backbone protects the glycosidic bond of this residue from cleavage by the EG. Removal of the *O*-acetyl substituents prior to EG-treatment of the AXG results in oligosaccharide fragments that are smaller than those produced by EG-treatment of the *O*-acetylated AXG. Therefore, analysis of the complex mixture of oligosaccharides obtained by EG-treatment of native tobacco AXGs provides information regarding the distribution of AXG side chains that would be lost if the AXG is de-*O*-acetylated prior to EG-treatment. Furthermore, the large library of oligosaccharide fragments generated by this approach revealed additional correlations between the structural features of AXGs and diagnostic chemical shift effects in their ^{1}H NMR spectra.

Keywords: Xyloglucan; Arabinoxyloglucan; Structural characterization; Tobacco; Tomato; Solanacea

1. Introduction

Xyloglucans are hemicellulosic polysaccharides present in the cell walls of virtually all higher plants. The xyloglucans of most dicotyledonous plants are highly branched polysaccharides in which approximately 75% of the (1 → 4)-linked β-D-Glc*p* residues in the backbone bear a glycosyl side chain at O-6 [1–7]. The glycosyl residue that is directly attached to O-6 of the branched β-D-Glc*p* residue is invariably α-D-Xyl*p* [1–7]. Up to 50% of side chains in the xyloglucans of most dicotyledonous plants contain more than one residue, due to the presence of β-D-Gal*p* or α-L-Fuc*p*-(1 → 2)-β-D-Gal*p* moieties at O-2 of the α-D-Xyl*p* residues. Xyloglucans produced by solanaceous plants are unusual in that only 40% of the β-D-Glc*p* residues in a typical solanaceous xyloglucan bear a glycosyl side chain at O-6 [8–11]. Furthermore, up to 60% of the α-D-Xyl*p* residues of solanaceous xyloglucans are substituted at O-2 with α-L-Ara*f* residues [8–11], and so these xyloglucans are appropriately called arabinoxyloglucans (AXGs). The AXGs of some solanaceous plants, such as potato, also have β-D-Gal*p* substituents [11] at O-2 of some of the α-D-Xyl*p* residues, but α-L-Fuc*p*-(1 → 2)-β-D-Gal*p* moieties have not been found in solanaceous AXGs.

Xyloglucans are structurally related to cellulose, but the presence of side chains at O-6 of their β-D-Glc*p* residues makes them very different from cellulose in terms of their physical properties. For example, xyloglucans bind tightly to cellulose, but are often soluble in aqueous media in the absence of cellulose. This property makes it possible for soluble xyloglucans, synthesized in the plant's Golgi apparatus, to be transported to the apoplastic space where they are incorporated into the xyloglucan–cellulose network [1]. The xyloglucan molecules in this network probably act as crosslinks between the cellulose microfibrils [1]. The xyloglucan crosslinks are accessible to endolytic enzymes that may facilitate cell-wall expansion by allowing the controlled slippage and reorientation of microfibrils in the network [1]. The susceptibility of individual β-D-Glc*p* residues in the backbone of a xyloglucan to enzymatic cleavage depends on the local side chain substitution pattern [2,4,5,12]. Thus, the side chain substitution patterns of xyloglucans are likely to have profound effects on their transport, their incorporation into the xyloglucan–cellulose network, and their subsequent metabolism in the plant's primary cell wall.

The relationships between the structure of xyloglucans and their capacity to function in the plant cell wall are not well understood. The cell walls of all higher plants thus far

studied (with the notable exception of the graminae) have xyloglucans with either α-L-Fuc*p*-(1 → 2)-β-D-Gal*p*-(1 → 2)-α-D-Xyl*p* or α-L-Ara*f*-(1 → 2)-α-D-Xyl*p* side chains, but not with both. The water solubility of xyloglucans is correlated to the presence of α-L-Ara*f* or α-L-Fuc*p*-(1 → 2)-β-D-Gal*p* moieties [10,13]. This suggests that the intact side chain structures are necessary for transport and incorporation of the xyloglucan into the cell wall. Thus, α-L-Ara*f* residues and α-L-Fuc*p*-(1 → 2)-β-D-Gal*p* moieties may be functionally interchangeable at some level. However, the distribution of oligoglycosyl side chain structures along the xyloglucan backbone is likely to have a significant effect on the physical properties of the polysaccharide. The distribution of oligoglycosyl side chains in the xyloglucans produced by non-solanaceous plants has been extensively studied [1,2,7]. Further knowledge of the side chain distribution in solanaceous AXGs is required to determine whether the oligoglycosyl side chains have similar functional roles in AXGs and fucosylated xyloglucans. The structural analyses described herein were performed in order to address this important question.

We have previously described [3–7] correlations between the structures of xyloglucan oligoglycosyl alditols and the chemical shifts of diagnostic resonances in their ^{1}H NMR spectra. The spectroscopic analyses described herein allowed us to expand our list of "structure–chemical shift correlations" (SCSCs) to include resonances diagnostic for the presence and location of arabinose-containing side chains in oligoglycosyl alditols derived from AXGs. These SCSCs are based on the structural analysis of oligosaccharides generated by endoglucanase treatment of tobacco AXG. In addition, we describe the structures of two oligosaccharides that embody structural features typical of tomato AXG, including the presence of β-Ara*f* residues, which have not been previously reported as components of xyloglucans.

2. Materials and methods

Preparation of AXGs.—Tobacco (*Nicotiana tabacum* L. cv Samsun) cells (isolated by Stefan Eberhard of the CCRC) were cultured in the medium of Linsmaier and Skoog [14] supplemented with 2,4-dichlorophenoxyacetic acid (2,4-D, 1 mg/mL) and sucrose (3%). Tomato (*Lycopersicon esculentum* 'Bonnie Best') cells [15] were cultured in MS medium [16]. Seven days after inoculation, cells were removed from 4 L of culture by filtration through sintered glass, and the culture filtrate was extensively dialyzed (Spectra-Por 6000–8000 MWCO tubing) vs. deionized water and then concentrated to approximately 200 mL by rotary evaporation. Eight volumes of abs ethanol were added to the retentate, and the precipitated polysaccharides were collected by centrifugation (20 min at 6000*g*). Acidic contaminants were removed by dissolving the pellet in 10 mM imidazole · HCl buffer, pH 7, and passing it through a column (20 mL) of Q-Sepharose (Phamacia), eluting with the same buffer. The column eluant, containing the AXG, was dialyzed vs. deionized water and lyophilized. The lyophilized material was dissolved (5 mg/mL) in deionized water and AXG was precipitated by addition of $(NH_4)_2SO_4$ to saturation (761 g/L) and chilling the solution (2 h, 0 °C). Precipitated AXG was collected by centrifugation (20 min at 10,000*g*), resuspended in water, dialyzed, and lyophilized, yielding 93 mg of tomato AXG and 55 mg of tobacco AXG.

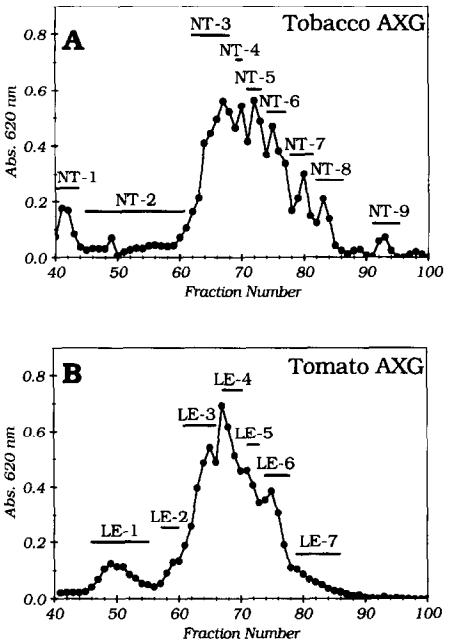

Fig. 1. Bio-Gel P-2 chromatography of oligosaccharides generated by EG treatment of AXG. Fractions NT-1 through NT-9 from tobacco (*Nicotiana tabacum*) AXG (A) and LE-1 through LE-7 from tomato (*Lycopersicon esculentum*) AXG (B) were pooled as indicated. The carbohydrate content of the fractions, expressed in optical absorbance units (620 nm), was determined by the anthrone assay [17].

Endoglucanase treatment of AXGs.—Tobacco AXG (55 mg) and tomato AXG (74 mg) were each dissolved in 100 mL of 10 mM sodium acetate buffer, pH 5.2, containing 0.02% thimerosal and 10 U of *endo*-(1 → 4)-β-D-glucanase (EC 3.2.1.4, Megazyme, Australia). The samples were incubated at room temperature for 48 h and then concentrated by rotary evaporation. Small amounts of insoluble material that appeared during the concentration step were removed by centrifugation (10 min at 1000 *g*). The supernatant solution was desalted on Sephadex G-10. AXG oligosaccharides were detected in the G-10 eluant by the anthrone assay for hexoses [17]. The salt-free fractions were pooled and lyophilized.

Gel-permeation chromatography.—AXG oligosaccharides were chromatographed on two Bio-Gel P-2 columns (−400 mesh, 90 × 1.6 cm) connected in series and eluted with deionized water [3]. Fractions (2.5 mL) were collected, assayed for carbohydrate content by the anthrone assay, and pooled as indicated in Fig. 1.

Reduction of oligosaccharides.—Partially purified AXG oligosaccharides recovered after Bio-Gel P-2 chromatography were converted to the corresponding oligoglycosyl alditol derivatives by reduction with $NaBH_4$ (10 mg/mL in M NH_4OH, 1 mL). After incubating the reaction for 1 h at room temperature, the solution was chilled (0 °C), and the remaining borohydride was converted to borate by dropwise addition of acetone (100 μL). The solvent was then evaporated, and the residue, containing oligoglycosyl

alditols, was dissolved in 0.5 mL of M NaH_2PO_4. The oligoglycosyl alditol solution was loaded onto an octadecyl silica cartridge (Supelclean LC-18, Supelco) that had been preconditioned by washing with 10 mL of methanol, followed by 10 mL of water. The loaded cartridge was washed with 4 mL of water to remove salts, including boron-containing compounds. The oligoglycosyl alditols were then eluted from the cartridge with 5 mL of 25% methanol.

Liquid chromatography of oligoglycosyl alditols.—Oligoglycosyl alditols were separated by reversed-phase HPLC on an octadecyl silica column (Hibar Lichrosorb RP-18, 0.25 × 25 cm). A typical chromatographic run involved the injection of 100 μL of sample and isocratic elution (1.0 mL/min) with aqueous methanol (see Table 1 below for details). Oligoglycosyl alditols were detected by monitoring the refractive index (RI) of the eluant. Individual RI peaks were pooled, and their purity was evaluated by ^1H NMR spectroscopy. When necessary, oligoglycosyl alditols were further separated by high-performance anion-exchange chromatography (HPAEC) with pulsed amperometric detection, using a Dionex CarboPac PA1 column (4 × 250 mm) eluted with a linear gradient (20 → 100 mM NaOAc in 100 mM NaOH over 15 min), followed by isocratic elution with 100 mM NaOAc in 100 mM NaOH for another 15 min. HPAEC fractions were collected and neutralized by bubbling CO_2 through the solution for ~ 1 min and then desalted by reversed-phase chromatography on an octadecyl silica cartridge, as described above (see Reduction of oligosaccharides section), except that no NaH_2PO_4 was added.

Glycosyl-linkage analysis.—Methylation of oligosaccharides and oligoglycosyl alditols was performed using the method of Ciucanu and Kerek [18], except that the suspension of NaOH in Me_2SO was prepared as described by Anumula and Taylor [19]. Partially methylated alditol acetate derivatives were prepared by standard methods [20] and analyzed by GLC–MS [20].

Matrix-assisted laser-desorption / ionization time-of-flight mass spectrometry (MALDITOFMS).—MALDITOF mass spectra were recorded as previously described [7] using a Hewlett–Packard LDI 1700 XP spectrometer and 2,4-dihydroxybenzoic acid as the matrix.

Fast-atom bombardment mass spectrometry (FABMS).—Oligoglycosyl alditols (20–200 μg) were per-*O*-acetylated with a mixture of trifluoroacetic anhydride and acetic acid [21] and dissolved in methanol (20 μL). An aliquot (1 μL) of this solution was mixed on the FAB-probe tip with 2 μL of either 1-thioglycerol or 3-nitrobenzyl alcohol (NBA). Mass spectra of the per-*O*-acetylated oligoglycosyl alditols were recorded with a JEOL (Tokyo, Japan) SX/SX102A tandem four-sector mass spectrometer operating at an accelerating potential of 10 kV. Fast xenon atoms were generated with a JEOL FAB gun operating at 6 kV. Spectra were recorded at a resolution of approximately 1000 in positive-ion mode, scanning from m/z 1 to m/z 2500 over 1 min with 100 Hz filtering. Average spectra consisting of 2 to 4 scans were generated with the JEOL complement data system.

FABMS/MS spectra were recorded as described for FABMS, except that 1 μL of the per-*O*-acetylated oligoglycosyl alditol solution, 1 μL of approximately 5% 18-crown-6 ether in methanol, and 2 μL of NBA were mixed on the probe tip [22]. Decomposition of the quasimolecular $[M + H]^+$ ion was induced by collision with He

gas in a cell between the two mass spectrometers. The electrical potential of the collision cell was held at 3 kV relative to the detector, resulting in a collision energy of 7 kV. The He pressure was adjusted to give 75% attenuation of the ion current, and daughter ions were analyzed in MS-2.

NMR spectroscopy.—Solutions of the oligoglycosyl alditols in deuterium oxide (99.6 atom% ^{2}H, Cambridge Isotope Laboratories, CIL) were lyophilized to remove exchangeable protons, and the residues were dissolved in D_2O (99.96% atom% ^{2}H, CIL). ^{1}H NMR spectra were recorded with a Bruker AM 500 spectrometer at ~299 K (reference HDO line at δ 4.75 ± 0.01 relative to internal acetone at δ 2.225). All 2D spectra (double-quantum filtered COSY [23], TOCSY [24], and ROESY [25]) were recorded using the time-proportional phase increment (TPPI) method [26] in both dimensions. The TOCSY mixing time was 170 ms and the ROESY mixing time was 250 ms.

3. Results and discussion

Isolation of AXGs.—AXGs were purified from the medium of suspension-cultured tobacco and tomato cells (see Materials and methods). Unlike most polysaccharides, AXGs from solanaceous plants are poorly soluble in saturated ammonium sulfate [10]. This property made it possible to separate the AXGs from other neutral polysaccharides, such as mannans, that are also secreted into the culture media of the tomato and tobacco cells. Other precipitation techniques were found to be less selective, and in some cases, to degrade the AXG. For example, the alkali-labile *O*-acetyl substituents of the AXG were hydrolyzed when mannans were removed by selective precipitation with $Ba(OH)_2$. The *O*-acetyl substituents survived when the AXG was selectively precipitated with ammonium sulfate.

Glycosyl composition analysis [20] of the ammonium sulfate precipitated tobacco AXG (data not shown) showed that it was free of mannan. Small amounts of mannose (3.1 mol%) and galactose (7.5 mol%) were present in the tomato AXG preparation, suggesting that some (galacto)mannan co-precipitated with the tomato AXG. However, further analysis of the tomato AXG (see below) showed that galactosyl residues are an integral part of its structure. Integration of anomeric proton resonances in the ^{1}H NMR spectra of the precipitated AXGs indicated that 40–45% of the β-D-Glc*p* residues in the tobacco AXG are branched, while 45–50% of the β-D-Glc*p* residues in the tomato AXG are branched. These results confirm that saturated ammonium sulfate selectively precipitates AXGs in the presence of mannans [10] and that AXGs have fewer branched Glc*p* residues in their backbones than do xyloglucans from non-solanaceous dicots [8,9,11].

Generation of AXG oligosaccharides and Bio-Gel P-2 chromatography.—Oligosaccharide subunits of the purified AXGs were generated by treatment with *endo*-β-(1 → 4)-D-glucanase (EG). Relatively simple mixtures of oligosaccharides are generated by EG-treatment of AXGs that have been extracted from the cell walls of solanaceous plants with strong alkali [8,9]. However, very complex mixtures of oligosaccharides are

generated by EG-treatment of the AXGs that were purified from the culture medium, as revealed by gel-permeation chromatography on Bio-Gel P-2 (Fig. 1). The presence of *O*-acetyl substituents at O-6 of some of the β-D-Glc*p* residues of the oligosaccharides in these complex mixtures was revealed by ^{1}H NMR and MALDITOFMS analyses (see below). We attribute the increased complexity to the inability of the EG to cleave the glycosidic bond of the 6-*O*-acetylated β-D-Glc*p* residues in the AXG backbone, resulting in the generation of larger, more complex oligosaccharide fragments (see below).

MALDITOFMS analysis of the P-2 fractions.—The presence of *O*-acetyl substituents in the oligosaccharides generated by EG-treatment of the tobacco and tomato AXGs was confirmed by MALDITOFMS. The considerable heterogeneity of the fractions obtained by Bio-Gel P-2 chromatography of these oligosaccharides was also revealed by this analysis. For example, 13 ions in the MALDITOF mass spectrum of fraction NT-3 (from tobacco AXG, Fig. 1A) and 19 ions in the MALDITOF spectrum of fraction LE-3 (from tomato AXG, Fig. 1B) were assigned as quasimolecular $[M + Na]^+$ ions of oligosaccharides. The masses of these ions indicate that hepta-, octa- and nona-saccharides are present in both fractions, and that the oligosaccharides in fraction NT-3 have up to 3 *O*-acetyl substituents, while those in Fraction LE-3 have no more than one *O*-acetyl substituent. Thus, the presence of *O*-acetyl substituents significantly increases the heterogeneity of the AXG oligosaccharides, especially those generated from tobacco AXG.

^{1}H NMR analysis of the Bio-Gel P-2 fractions.—The ^{1}H NMR spectra of the Bio-Gel P-2 fractions included singlet resonances at approximately δ 2.15, assigned as the methyl protons of the *O*-acetyl substituents. These spectra also included signals at δ 4.31 (dd, $^3J_{5,6}$ 5, $^3J_{6,6'}$ 12 Hz) and δ 4.62 (dd, $^3J_{5,6'} < 2$, $^3J_{6,6'}$ 12 Hz) that were assigned as H-6 and H-6′ of β-Glc*p* residues substituted at O-6 with an *O*-acetyl group. These assignments were confirmed by analysis of the 2D TOCSY spectrum of fraction LE-4 (data not shown), which indicated that the resonances at δ 4.31 and δ 4.62 belonged to a *J*-coupled spin system corresponding to a β-Glc*p* residue (H-1 δ 4.55, $^3J_{1,2}$ 8 Hz). Furthermore, removal of the *O*-acetyl substituents of the oligosaccharides by reduction with $NaBH_4$ resulted, as expected, in the disappearance of the resonances at δ 2.15, δ 4.31 and δ 4.62. Although *O*-acetyl substituents have been found on the side chains of xyloglucans from non-solanaceous plants [27], this is the first observation of *O*-acetyl substituents on β-D-Glc*p* residues in the backbone of any xyloglucan.

Typically, fungal EGs can only hydrolyze the glycosidic bonds of unbranched β-Glc*p* residues in the backbone of substituted β-(1 → 4)-linked glucans (such as AXGs). That is, a substituent at any position except O-4 of the β-Glc*p* residue renders its glycosidic bond much less susceptible to hydrolysis by the fungal EG [2,12]. Therefore, stretches of unbranched (1 → 4)-linked β-Glc*p* residues in the backbones of AXGs produced by solanaceous plants would probably be susceptible to cleavage by the fungal EG if O-6 of these residues were not *O*-acetylated. Extraction of AXGs with strong alkali removes *O*-acetyl substituents, increasing the susceptibility of the AXG backbone to hydrolysis by the fungal EG. However, the EG-resistance of *O*-acetylated β-D-Glc*p* residues in the AXG backbone leads to a mixture of relatively large, complex oligosaccharides when the native AXG is treated with EG.

Isolation of oligoglycosyl alditols.—Further analysis of the structures of the oligosaccharides generated by EG-treatment of the AXGs required separation of the complex mixtures obtained by Bio-Gel P-2 chromatography. The separation and structural analysis of xyloglucan oligosaccharides is facilitated by first converting them to the corresponding oligoglycosyl alditol derivatives [3–7]. This step greatly reduces the chemical heterogeneity of the mixture by removing the *O*-acetyl substituents and converting mutarotational isomers to a single form. The Bio-Gel P-2 fractions were therefore reduced with borohydride, and then subjected to reversed-phase HPLC on ODS. Several fractions obtained by reversed-phase HPLC still contained mixtures of oligoglycosyl alditols that were resolved by HPAEC. The characteristics of the AXG oligoglycosyl alditols purified by these techniques are listed in Table 1.

HPLC and HPAEC of the tobacco AXG oligoglycosyl alditols from P-2 fractions NT-3 through NT-7 yielded 38 subfractions, containing 22 unique oligoglycosyl alditols (Fig. 2, Table 1). The structures of 20 of these oligoglycosyl alditols were completely determined. The mixtures of oligoglycosyl alditols obtained from tomato AXG were even more heterogeneous, due to the presence of additional side chain structures not present in the tobacco AXG oligoglycosyl alditols. Two novel oligoglycosyl alditols (LXGGol and GXTGol, Fig. 1) derived from tomato AXG were structurally characterized. Isolation and characterization of the complete set of the tomato AXG oligoglycosyl alditols is in progress.

NMR analysis of tobacco AXG oligoglycosyl alditols.—The availability of a large number of closely related and highly purified tobacco AXG oligoglycosyl alditols made it possible to derive a self-consistent set of structural and spectral assignments for these molecules. The structures of the oligoglycosyl alditols in the 38 subfractions obtained by HPLC and HPAEC were initially deduced by analysis of their ^{1}H NMR spectra. This analysis involved the utilization of previously described correlations (SCSCs) between the structural features of xyloglucan oligoglycosyl alditols and the chemical shifts of diagnostic resonances in their ^{1}H NMR spectra [3–7]. Application of these SCSCs made it possible to determine the structure and location of side chains of several novel oligoglycosyl alditols, including XGGGol, XXGGol, GXXGGol, XSGol, SXGol, SSGol, and SSGGol. A comparative examination of the ^{1}H NMR spectra of these novel oligoglycosyl alditols revealed novel SCSCs. The application of these newly observed SCSCs to the ^{1}H NMR spectra of the remaining tobacco AXG oligoglycosyl alditols provided enough additional information to allow their structures to be assigned as well. The results are self-consistent in that application of the complete set of SCSCs to the complete set of ^{1}H NMR spectra do not lead to any structural inconsistencies. Nevertheless, these analyses do not, in themselves, constitute unambiguous proofs of the structures of the oligoglycosyl alditols. Therefore, the structural assignments were confirmed by other techniques (see below), thus validating the ^{1}H NMR assignments and the SCSCs upon which they are based. This general approach is illustrated in the following paragraphs, using the ^{1}H NMR spectra of several oligoglycosyl alditols as examples.

^{1}H NMR analysis of fraction NT-7-4 (XSGol).—The oligoglycosyl alditol in fraction NT-7-4 was assigned the structure XSGol on the basis of its 1D and 2D ^{1}H NMR spectra (Fig. 3, Table 2). The isolated *J*-coupled spin systems that correspond to

Table 1
Characteristics of oligoglycosyl alditols from tobacco AXG

Fraction [a]	Chromatographic behavior (method) [b]	Recovery % of AXG [c]	Fraction content [d]	$[M+Na]^+$ chemical mass [e]
NT-3	Fig. 1 (P-2)	30.2 [f]	See below [g]	–
NT-3-1	10.4 min (ODS, 6.5%)	1.3	GSGGGol	1119.3 (1118.0)
NT-3-2	16.0 min (ODS, 6.5%)	1.3	50% XSGGol	1089.3 (1087.9)
NT-3-3	17.8 min (ODS, 6.5%)	6.1	See below [g]	–
NT-3-3-1	15.3 min (HPAEC)	2.7	XXGGGol	1119.1 (1118.0)
NT-3-3-2	19.5 min (HPAEC)	3.4	GXSGGol	1250.1 (1250.1)
NT-3-4	22.3 min (ODS, 6.5%)	2.2	GSSGGol	1382.4 (1382.2)
NT-3-5	23.7 min (ODS, 6.5%)	19.2	XSGGGol	1250.3 (1250.1)
NT-4	Fig. 1 (P-2)	12.7 [f]	See below [g]	–
NT-4-1	8.6 min (ODS, 6.5%)	0.9	SGGGol	956.7 (955.8)
NT-4-2	16.0 min (ODS, 6.5%)	7.7	XSGGol	1088.7 (1087.9)
NT-4-3	19.0 min (ODS, 6.5%)	3.4	See below [g]	–
NT-4-3-1	15.3 min (HPAEC)	1.2	XXGGGol	1119.4 (1118.0)
NT-4-3-2	18.2 min (HPAEC)	0.7	SXGGol	1088.2 (1087.9)
NT-4-3-3	19.3 min (HPAEC)	1.4	GXSGGol	1251.1 (1250.1)
NT-4-4	26.8 min (ODS, 6.5%)	0.6	SSGGol	1222.3 (1220.1)
NT-5	Fig. 1 (P-2)	18.4 [f]	See below [g]	–
NT-5-1	6.1 min (ODS, 6.0%)	0.2	Mixture	–
NT-5-2	6.9 min (ODS, 6.0%)	1.0	GSGGol	956.6 (955.8)
NT-5-3	8.0 min (ODS, 6.0%)	0.4	Weak	–
NT-5-4	8.6 min (ODS, 6.0%)	1.2	SGGGol	956.5 (955.8)
NT-5-5	9.7 min (ODS, 6.0%)	1.6	GXSGol	1089.0 (1087.9)
NT-5-6	12.2 min (ODS, 6.0%)	1.5	Mixture	–
NT-5-7	14.1 min (ODS, 6.0%)	0.7	GXXGGol	1119.5 (1118.0)
NT-5-8	15.7 min (ODS, 6.0%)	10.0	XSGGol	1090.7 (1087.9)

Table 1 (continued)

Fraction [a]	Chromatographic behavior (method) [b]	Recovery % of AXG [c]	Fraction content [d]	$[M+Na]^+$ chemical mass [e]
NT-5-9	19.8 min (ODS, 6.0%)	1.0	SXGGol	1089.2 (1087.9)
NT-5-10	23.4 min (ODS, 6.0%)	0.7	See text [h]	1087.7 (1087.9)
NT-6	Fig. 1 (P-2)	19.6 [f]	See below [g]	–
NT-6-1	7.8 min (ODS, 5.0%)	2.3	See below [g]	–
NT-6-1-1	10.6 min (HPAEC)	1.1	XGGGol	822.2 (823.7)
NT-6-1-2	13.3 min (HPAEC)	1.2	SGGol	790.4 (793.7)
NT-6-2	9.9 min (ODS, 5.0%)	1.3	GSGGol	957.0 (955.8)
NT-6-3	11.5 min (ODS, 5.0%)	6.2	XSGol	926.0 (925.8)
NT-6-4	14.0 min (ODS, 5.0%)	0.5	70% SXGol	927.3 (925.8)
NT-6-5	15.0 min (ODS, 5.0%)	1.7	GXSGol	1089.2 (1087.9)
NT-6-6	18.2 min (ODS, 5.0%)	6.8	See below [g]	–
NT-6-6-1	11.0 min (HPAEC)	5.9	XXGGol	956.6 (955.8)
NT-6-6-2	18.7 min (HPAEC)	0.9	SSGol	1060.2 (1057.9)
NT-6-7	27.9 min (ODS, 5.0%)	0.8	XSGGol	1089.7 (1087.9)
NT-7	Fig. 1 (P-2)	10.4 [f]	See below [g]	–
NT-7-1	5.4 min (ODS, 5.0%)	0.9	See below [g]	–
NT-7-1-1	6.7 min (HPAEC)	0.3	Weak	–
NT-7-1-2	12.8 min (HPAEC)	0.6	GSGol	790.1 (793.7)
NT-7-2	8.1 min (ODS, 5.0%)	1.7	SGGol	790.3 (793.7)
NT-7-3	8.7 min (ODS, 5.0%)	0.4	XXGol SGGol	790.9 (793.7)
NT-7-4	11.9 min (ODS, 5.0%)	6.5	XSGol	926.0 (925.8)
NT-7-5	14.8 min (ODS, 5.0%)	0.4	SXGol	926.6 (925.8)
NT-7-6	16.0 min (ODS, 5.0%)	0.4	See text [h]	925.9 (925.8)
NT-8	Fig. 1 (P-2)	6.8 [f]	Mixture [i]	789.5 (791.7) [i]
NT-9	Fig. 1 (P-2)	1.9 [f]	Mixture [j]	–

individual glycosyl residues in this oligoglycosyl alditol were identified by analyses of its COSY and TOCSY spectra. The resonance ($^3J_{1,2}$ 1.7 Hz) at δ 5.172 was assigned as H-1 of a terminal α-L-Ara*f* residue by its diagnostic chemical shift [8] and by the coupling pattern of its associated spin system [5] (Tables 2 and 3). The α-anomeric resonance ($^3J_{1,2}$ 3.7 Hz) at δ 4.938, *J*-coupled to an H-2 resonance ($^3J_{2,3}$ 10 Hz) at δ 3.545, is diagnostic for a terminal α-D-Xyl*p* residue attached to the 6-substituted β-D-Glc*p* at the non-reducing end of the main chain [3–7]. The α-anomeric resonance ($^3J_{1,2}$ 3.7 Hz) at δ 5.088 coupled to an H-2 resonance ($^3J_{2,3}$ 10 Hz) at δ 3.579 is consistent with the presence of an α-D-Xyl*p* residue substituted at *O*-2 with an α-L-Ara*f* residue [3,8]. The resonance at δ 4.617 ($^3J_{1,2}$ 8 Hz) was assigned as H-1 of a 4,6-substituted β-D-Glc*p* residue linked directly to the alditol by virtue of its characteristic downfield shift [3–7]. The resonance at δ 4.550 ($^3J_{1,2}$ 8 Hz) was assigned as H-1 of a 6-substituted β-D-Glc*p* residue at the end of the main chain by virtue of the characteristic upfield shift [3–7] of the H-2 resonance (δ 3.329). The only structure consistent with this set of resonance assignments is XSGol (Fig. 2).

Notes to Table 1:

[a] Fraction names are hierarchical. For example, NT-3, obtained by Bio-Gel P-2 chromatography, was reduced and then fractionated by reversed-phase HPLC to yield fractions NT-3-1 through NT-3-5. Fractions NT-3-3-1 and NT-3-3-2 were obtained by HPAEC of NT-3-3.

[b] The retention time of each fraction is given, except for fractions obtained by Bio-Gel P-2 chromatography, shown in Fig. 1. The last chromatographic step in the purification of the fraction is indicated in parentheses. ODS refers to reversed-phase HPLC with isocratic elution using aq methanol at the indicated concentration. Other chromatographic conditions are given in Materials and methods section.

[c] Values for the net recovery (% of AXG) for each fraction were calculated as follows. First, the amount of material in each fraction was expressed as a percent of the material recovered when its parent fraction was separated by the chromatographic technique. This quantity was multiplied by the amount of material in the parent fraction, expressed in the same way. For example, fraction NT-3-1 comprised 4.4% of the material recovered during reversed-phase HPLC of Fraction NT-3. Therefore, fraction NT-3-1 was estimated to comprise (30.2% × 4.4%) = 1.32% of the AXG. The total recovery of each oligoglycosyl alditol is given in Fig. 2. For example, XXGGGol (3.9% of AXG) was recovered in fractions NT-3-3-1 (2.7% of AXG) and NT-4-3-1 (1.2% of AXG).

[d] Specific structures are indicated using the nomenclature of Fig. 2 when one oligoglycosyl alditol accounts for more than 85% of the fraction, unless otherwise noted.

[e] The chemical mass of the $[M+Na]^+$ ion of the most abundant component in each fraction was determined by MALDITOFMS. The calculated chemical mass for each assigned structure is in parentheses.

[f] Fractions NT-3 through NT-9 contained nearly all of the AXG oligosaccharides recovered from the Bio-Gel P-2 column, and so the listed values are normalized such that the recoveries for these seven fractions add up to 100%.

[g] Heterogeneous column fractions were further separated by complementary chromatographic methods, and contents of the highly purified subfractions are given in entries that immediately follow in the table.

[h] The structures of the unusual oligoglycosyl alditols in fractions NT-5-10 and NT-7-6 could not be completely determined, due to insufficient material (see text).

[i] Fraction NT-8 was not reduced before MALDITOF analysis. The most abundant ion (*m*/*z* 789.5) in the MALDITOF mass spectrum of this fraction corresponds in mass to hexose$_3$pentose$_2$. The ^{1}H NMR spectrum indicated that the most abundant oligomer (~ 60%) in this fraction is XXG (i.e., XXGol after reduction).

[j] Fraction NT-9 contained low-mass oligosaccharides whose $[M+Na]^+$ ions were obscured by matrix ions in the MALDITOF mass spectrum. However, ^{1}H NMR analysis of reduced NT-9 indicated its major component (~ 50%) is XGol.

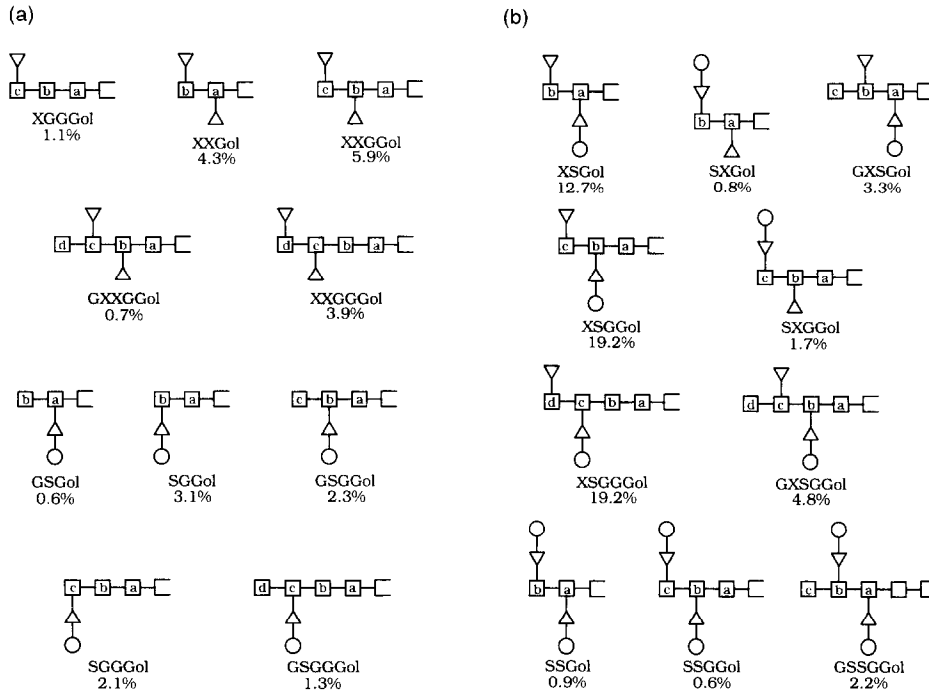

Key for Glycosyl Residues

□— = β-D-Glc*p*-(1→4)- ⌐ = D-Glcol

○ = α-L-Ara*f*-(1→2)- △ = α-D-Xyl*p*-(1→6)-

■ = β-D-Gal*p*-(1→2)- ● = β-Ara*f*-(1→3)-

One Letter Code for Substitution Patterns

G ≡ β-D-Glc*p* **Gol** ≡ D-Glcol

X ≡ α-D-Xyl*p*-(1→6)-β-D-Glc*p*

S ≡ α-L-Ara*f*-(1→2)-α-D-Xyl*p*-(1→6)-β-D-Glc*p*

T ≡ β-Ara*f*-(1→3)-α-L-Ara*f*-(1→2)-α-D-Xyl*p*-(1→6)-β-D-Glc*p*

L ≡ β-D-Gal*p*-(1→2)-α-D-Xyl*p*-(1→6)-β-D-Glc*p*

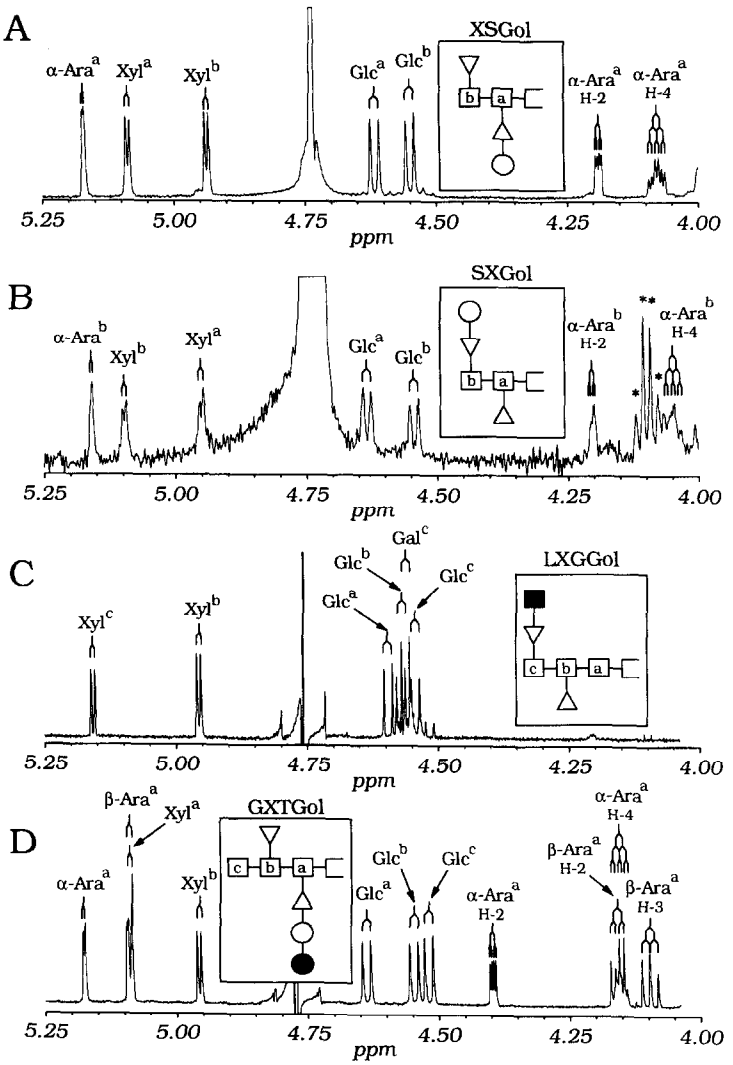

Fig. 3. Downfield region of the ^{1}H NMR spectra of four purified oligoglycosyl alditols. (A) XSGol, fraction NT-6-3; (B) SXGol, fraction NT-7-5; (C) LXGGol, fraction LE-3-4-2; (D) GXTGol, fraction LE-3-4-3. Structures are indicated and glycosyl residues are distinguished as described in Fig. 2 and footnote b of Table 2. All indicated resonances are assigned as H-1, except where noted otherwise. The H-4 resonance (δ 4.055) of α-L-Ara*f* in the spectrum of SXGol (B) is obscured by H-2 of lactic acid, a common contaminant.

Fig. 2. Structures of the oligoglycosyl alditols obtained from tobacco and tomato AXG. Oligoglycosyl alditol structures are indicated using an uppercase letter to represent each β-D-Glc*p* residue and its pendant side chains, as described [31]. Each β-D-Glc*p* residue and the glycosyl residues of its pendant side chain are distinguished by a lower case letter that indicates the location of the β-D-Glc*p* residue vis a vis the alditol moiety, as described in footnote b of Table 2. The estimated proportion of tobacco AXG represented by each oligoglycosyl alditol is also indicated.

Table 2
^{1}H NMR chemical shifts [a] of AXG oligoglycosyl alditols

Linkage	Residue	Site [b]	H-1	H-2	H-3	H-4	H-5	H-5′	H-6	H-6′
XGGGol										
T	α-D-Xyl*p*	c	4.940	*** [c]	***	***	***	***	–	–
6	β-D-Glc*p*	c	4.539	3.330	***	***	***	–	***	***
4	β-D-Glc*p*	b	4.546	3.37	***	***	***	–	***	***
4	β-D-Glc*p*	a	4.592	3.37	***	***	***	–	***	***
XXGGol										
T	α-D-Xyl*p*	c	4.941	3.543	3.733	***	***	***	–	–
T	α-D-Xyl*p*	b	4.957	3.544	3.726	***	***	***	–	–
6	β-D-Glc*p*	c	4.554	3.339	3.52	3.52	3.70	–	3.780	3.936
4,6	β-D-Glc*p*	b	4.567	3.389	3.667	3.736	3.826	–	3.902	4.005
4	β-D-Glc*p*	a	4.596	3.384	3.645	3.688	3.583	–	3.854	3.958
GXXGGol										
T	α-D-Xyl*p*	c	4.957	***	***	***	***	***	–	–
T	α-D-Xyl*p*	b	4.957	***	***	***	***	***	–	–
T	β-D-Glc*p*	d	4.516	3.322	3.507	3.411	3.49	–	***	***
4,6	β-D-Glc*p*	c	4.57	***	***	***	***	–	***	***
4,6	β-D-Glc*p*	b	4.57	***	***	***	***	–	***	***
4	β-D-Glc*p*	a	4.595	***	***	***	***	–	***	***
XXGGGol										
T	α-D-Xyl*p*	d	4.940	***	***	***	***	***	–	–
T	α-D-Xyl*p*	c	4.957	***	***	***	***	***	–	–
6	β-D-Glc*p*	d	4.555	3.339	***	***	***	–	***	***
4,6	β-D-Glc*p*	c	4.555	***	***	***	***	–	***	***
4	β-D-Glc*p*	b	4.544	***	***	***	***	–	***	***
4	β-D-Glc*p*	a	4.591	***	***	***	***	–	***	***
GSGol										
T	α-L-Ara*f*	a	5.171	4.193	***	4.078	***	***	–	–
2	α-D-Xyl*p*	a	5.091	***	***	***	***	***	–	–
T	β-D-Glc*p*	b	4.522	3.312	3.504	3.415	3.478	–	***	***
4,6	β-D-Glc*p*	a	4.614	3.405	***	***	***	–	***	***
SGGol										
T	α-L-Ara*f*	b	5.159	4.198	***	4.058	***	***	–	–
2	α-D-Xyl*p*	b	5.094	***	***	***	***	***	–	–
6	β-D-Glc*p*	b	4.533	3.331	3.517	3.464	***	–	***	***
4	β-D-Glc*p*	a	4.597	3.384	***	***	***	–	***	***
GSGGol										
T	α-L-Ara*f*	b	5.169	4.197	3.93	4.081	3.71	***	–	–
2	α-D-Xyl*p*	b	5.094	3.568	***	***	***	***	–	–
T	β-D-Glc*p*	c	4.510	3.314	3.504	3.414	3.480	–	***	***
4,6	β-D-Glc*p*	b	4.547	3.390	***	***	***	–	***	***
4	β-D-Glc*p*	a	4.597	3.390	***	***	***	–	***	***
SGGGol										
T	α-L-Ara*f*	c	5.158	4.197	***	4.056	***	***	–	–
2	α-D-Xyl*p*	c	5.096	***	***	***	***	***	–	–

Table 2 (continued)

Linkage	Residue	Site [b]	H-1	H-2	H-3	H-4	H-5	H-5′	H-6	H-6′
6	β-D-Glc*p*	c	4.522	3.338	3.515	3.464	* * *	–	* * *	* * *
4	β-D-Glc*p*	b	4.544	3.37	* * *	* * *	* * *	–	* * *	* * *
4	β-D-Glc*p*	a	4.592	3.37	* * *	* * *	* * *	–	* * *	* * *
GSGGGol										
T	α-L-Ara*f*	c	5.168	4.197	* * *	4.082	* * *	* * *	–	–
2	α-D-Xyl*p*	c	5.096	* * *	* * *	* * *	* * *	* * *	–	–
T	β-D-Glc*p*	d	4.509	3.312	3.503	3.413	3.477	–	* * *	* * *
4,6	β-D-Glc*p*	c	4.535	3.390	* * *	* * *	* * *	–	* * *	* * *
4	β-D-Glc*p*	b	4.544	3.373	* * *	* * *	* * *	–	* * *	* * *
4	β-D-Glc*p*	a	4.592	3.373	* * *	* * *	* * *	–	* * *	* * *
XSGol										
T	α-L-Ara*f*	a	5.172	4.191	3.940	4.079	3.714	3.85	–	–
T	α-D-Xyl*p*	b	4.938	3.545	3.736	* * *	* * *	* * *	–	–
2	α-D-Xyl*p*	a	5.088	3.579	3.785	* * *	* * *	* * *	–	–
6	β-D-Glc*p*	b	4.550	3.329	3.53	3.52	3.689	–	3.777	3.942
4,6	β-D-Glc*p*	a	4.617	3.411	3.67	3.66	3.78	–	3.93	3.99
SXGol										
T	α-L-Ara*f*	b	5.159	4.203	* * *	4.05	* * *	* * *	–	–
2	α-D-Xyl*p*	b	5.097	* * *	* * *	* * *	* * *	* * *	–	–
T	α-D-Xyl*p*	a	4.952	* * *	* * *	* * *	* * *	* * *	–	–
6	β-D-Glc*p*	b	4.544	3.343	* * *	3.465	* * *	–	* * *	* * *
4,6	β-D-Glc*p*	a	4.634	3.412	* * *	* * *	* * *	–	* * *	* * *
GXSGol										
T	α-L-Ara*f*	a	5.171	4.192	* * *	4.079	* * *	* * *	–	–
T	α-D-Xyl*p*	b	4.955	* * *	* * *	* * *	* * *	* * *	–	–
2	α-D-Xyl*p*	a	5.086	* * *	* * *	* * *	* * *	* * *	–	–
T	β-D-Glc*p*	c	4.518	3.322	3.507	3.414	3.49	* * *	–	–
4,6	β-D-Glc*p*	b	4.565	3.39	* * *	* * *	* * *	–	* * *	* * *
4,6	β-D-Glc*p*	a	4.619	3.39	* * *	* * *	* * *	–	* * *	* * *
XSGGol										
T	α-L-Ara*f*	b	5.169	4.197	3.933	4.082	3.711	3.846	–	–
T	α-D-Xyl*p*	c	4.939	3.546	3.732	* * *	* * *	* * *	–	–
2	α-D-Xyl*p*	b	5.093	3.571	3.853	* * *	* * *	* * *	–	–
6	β-D-Glc*p*	c	4.542	3.331	3.52	3.51	3.70	–	3.776	3.940
4,6	β-D-Glc*p*	b	4.551	3.395	3.67	3.69	3.85	–	3.95	3.95
4	β-D-Glc*p*	a	4.595	3.388	3.645	3.685	3.58	–	3.853	3.958
SXGGol										
T	α-L-Ara*f*	c	5.160	4.201	* * *	4.056	* * *	* * *	–	–
2	α-D-Xyl*p*	c	5.098	* * *	* * *	* * *	* * *	* * *	–	–
T	α-D-Xyl*p*	b	4.953	* * *	* * *	* * *	* * *	* * *	–	–
6	β-D-Glc*p*	c	4.528	3.341	3.518	3.467	* * *	–	* * *	* * *
4,6	β-D-Glc*p*	b	4.567	3.39	* * *	* * *	* * *	–	* * *	* * *
4	β-D-Glc*p*	a	4.596	3.39	* * *	* * *	* * *	–	* * *	* * *
XSGGGol										
T	α-L-Ara*f*	c	5.169	4.196	3.933	4.081	3.710	3.845	–	–

Table 2 (continued)

Linkage	Residue	Site [b]	H-1	H-2	H-3	H-4	H-5	H-5′	H-6	H-6′
T	α-D-Xyl*p*	d	4.938	3.550	3.733	* * *	* * *	* * *	–	–
2	α-D-Xyl*p*	c	5.095	3.572	3.850	* * *	* * *	* * *	–	–
6	β-D-Glc*p*	d	4.542	3.330	3.53	3.51	3.687	–	3.744	3.938
4,6	β-D-Glc*p*	c	4.542	3.394	3.67	3.69	3.85	–	3.95	3.95
4	β-D-Glc*p*	b	4.542	3.374	3.65	3.70	* * *	–	3.82	3.97
4	β-D-Glc*p*	a	4.591	3.374	3.642	3.686	3.577	–	3.855	3.960
GXSGGol										
T	α-L-Ara*f*	b	5.168	4.197	3.933	4.082	3.71	3.85	–	–
T	α-D-Xyl*p*	c	4.957	3.545	3.73	* * *	* * *	* * *	–	–
2	α-D-Xyl*p*	b	5.090	3.572	3.85	* * *	* * *	* * *	–	–
T	β-D-Glc*p*	d	4.517	3.321	3.506	3.413	3.485	–	3.733	3.916
4,6	β-D-Glc*p*	c	4.558	3.384	* * *	* * *	* * *	–	* * *	* * *
4,6	β-D-Glc*p*	b	4.552	3.396	* * *	* * *	* * *	–	* * *	* * *
4	β-D-Glc*p*	a	4.595	3.388	* * *	* * *	* * *	–	* * *	* * *
SSGol										
T	α-L-Ara*f*	b	5.158	4.196	* * *	* * *	* * *	* * *	–	–
T	α-L-Ara*f*	a	5.169	4.195	* * *	* * *	* * *	* * *	–	–
2	α-D-Xyl*p*	b	5.095	* * *	* * *	* * *	* * *	* * *	–	–
2	α-D-Xyl*p*	a	5.087	* * *	* * *	* * *	* * *	* * *	–	–
6	β-D-Glc*p*	b	4.521	3.327	* * *	* * *	* * *	–	* * *	* * *
4,6	β-D-Glc*p*	a	4.622	* * *	* * *	* * *	* * *	–	* * *	* * *
SSGGol										
T	α-L-Ara*f*	c	5.158	4.199	* * *	4.054	* * *	* * *	–	–
T	α-L-Ara*f*	b	5.167	4.199	* * *	4.080	* * *	* * *	–	–
2	α-D-Xyl*p*	c	5.097	* * *	* * *	* * *	* * *	* * *	–	–
2	α-D-Xyl*p*	b	5.090	* * *	* * *	* * *	* * *	* * *	–	–
6	β-D-Glc*p*	c	4.515	3.331	3.514	3.464	* * *	–	* * *	* * *
4,6	β-D-Glc*p*	b	4.553	3.39	* * *	* * *	* * *	–	* * *	* * *
4	β-D-Glc*p*	a	4.595	3.39	* * *	* * *	* * *	–	* * *	* * *
GSSGGol										
T	α-L-Ara*f*	c	5.168	4.200	* * *	4.077	* * *	* * *	–	–
T	α-L-Ara*f*	b	5.168	4.200	* * *	4.077	* * *	* * *	–	–
2	α-D-Xyl*p*	c	5.095	* * *	* * *	* * *	* * *	* * *	–	–
2	α-D-Xyl*p*	b	5.087	* * *	* * *	* * *	* * *	* * *	–	–
T	β-D-Glc*p*	d	4.509	3.311	3.503	3.412	3.477	–	* * *	* * *
4,6	β-D-Glc*p*	c	4.526	3.39	* * *	* * *	* * *	–	* * *	* * *
4,6	β-D-Glc*p*	b	4.554	3.39	* * *	* * *	* * *	–	* * *	* * *
4	β-D-Glc*p*	a	4.596	3.39	* * *	* * *	* * *	–	* * *	* * *
GXTGol										
T	β-Ara*f*	a	5.089	4.159	4.097	3.909	3.737	3.824	–	–
3	α-L-Ara*f*	a	5.175	4.397	3.974	4.153	3.731	3.857	–	–
T	α-D-Xyl*p*	b	4.957	3.543	3.725	* * *	* * *	* * *	–	–
2	α-D-Xyl*p*	a	5.088	3.572	3.76	* * *	* * *	* * *	–	–
T	β-D-Glc*p*	c	4.519	3.322	3.506	3.410	3.486	–	3.731	3.915
4,6	β-D-Glc*p*	b	4.547	3.383	3.657	3.739	3.801	–	3.889	4.017
4,6	β-D-Glc*p*	a	4.638	3.412	3.663	3.631	3.804	–	3.895	3.977

Table 2 (continued)

Linkage	Residue	Site [b]	H-1	H-2	H-3	H-4	H-5	H-5′	H-6	H-6′
LXGGol										
T	β-D-Galp	c	4.562	3.613	* * *	3.924	* * *	–	* * *	* * *
2	α-D-Xyl*p*	c	5.158	3.685	3.915	* * *	3.563	* * *	–	–
T	α-D-Xyl*p*	b	4.957	3.544	3.732	* * *	* * *	* * *	–	–
6	β-D-Glc*p*	c	4.544	3.345	3.520	3.458	3.744	–	3.813	3.883
4.6	β-D-Glc*p*	b	4.572	3.402	3.688	3.75	3.831	–	3.900	4.011
4	β-D-Glc*p*	a	4.596	3.384	3.650	3.691	3.586	–	3.856	3.960

[a] Chemical shifts in ppm relative to internal acetone at δ 2.225.

[b] The location of the residue vis a vis the D-glucitol moiety is indicated by a superscript lowercase letter. Thus, the backbone β-D-Glc*p* residues are designated Glc[c] → Glc[b] → Glc[a] → Glcol. Specific side chain residues are indicated by using the letter of the Glc*p* residue to which the side chain is attached. For example, Glc[a] is linked directly to O-4 of the glucitol moiety and Xyl[a] (when present) is linked to O-6 of Glc[a].

[c] Resonances that were not assigned are indicated by asterisks.

^{1}H NMR analysis of fraction NT-7-5 (SXGol).—Comparison of the ^{1}H NMR spectra of fractions NT-7-4 and NT-7-5 (Fig. 3) indicates that the oligoglycosyl alditols in these two fractions are isomers. Fraction NT-7-5 did not contain sufficient material to record 2D spectra. However, the oligoglycosyl alditol in this fraction was assigned the structure SXGol by comparing its 1D spectrum to that of NT-7-4 (XSGol) in light of previously observed SCSCs [3–7]. This analysis indicates that fraction NT-7-5 contains an oligoglycosyl alditol consisting of a 4,6-substituted β-D-Glc*p* residue (H-1 δ 4.634, $^3J_{1,2}$ 8 Hz) attached directly to a glucitol residue, a 6-substituted β-D-Glc*p* residue (H-1 δ 4.544, $^3J_{1,2}$ 8 Hz), an α-D-Xyl*p* side chain (H-1 δ 4.952, $^3J_{1,2}$ 4 Hz), and an α-L-Ara*f*-(1 → 2)-α-D-Xyl*p* side chain (α-Ara*f* H-1 δ 5.159, $^3J_{1,2}$ 2 Hz, α-Xyl*p* H-1

Table 3
Homonuclear scalar coupling constants [a] for α- and β-Ara*f* residues

Coupling constant	XXFGAXXGol [b]	XSGol [c]	GXTGol [c]		HypAra$_3$ [d]	
	Terminal α-Ara*f*	Terminal α-Ara*f*	3-Linked α-Ara*f*	Terminal β-Ara*f*	Various [d] β-Ara*f*	
$^3J_{1,2}$	1.8	1.8	1.8	4.7	4.2 → 4.6	
$^3J_{2,3}$	3.8	3.9	3.7	8.0	8.0 → 8.2	
$^3J_{3,4}$	6	6	6.8	7.3	7.1 → 7.3	

[a] Coupling constants in Hz. The constants $^3J_{4,5}$ and $^3J_{4,5'}$ reflect the rotational state of the exocyclic hydroxymethyl group, and therefore do not distinguish α- and β-Ara*f* residues. These parameters do not vary significantly for the Ara*f* residues listed in this table, with $^3J_{4,5} \approx 6–7$ and $^3J_{4,5'} \approx 3$ Hz.

[b] The reference oligoglycosyl alditol XXFGAXXGol was obtained [4,5] from the xyloglucan secreted by suspension-cultured sycamore cells.

[c] The anomeric configurations of the Ara*f* residues of XSGol and GXTGol, purified as described herein, were assigned by comparing their vicinal coupling constants to those measured for the Ara*f* residues of several known standards, including XXFGAXXGol and HypAra$_3$.

[d] The reference arabinoside HypAra$_3$ [36,37] was isolated from base-hydrolyzed cell walls of suspension-cultured sycamore cells. The range of coupling constant values for the three β-Ara*f* residues in the arabinoside are given.

δ 5.097, $^{3}J_{1,2}$ 4 Hz). Previous studies [3–7] have established that H-1 of a terminal α-D-Xyl$p$ residue is at δ 4.940 $\pm$ 0.003 when the α-D-Xyl$p$ residue is linked to O-6 of a 6-substituted β-D-Glc$p$ residue (as in XSGol). However, the H-1 chemical shift of the terminal α-D-Xyl$p$ residue of NT-7-5 is at δ 4.952, indicating that this residue is linked to O-6 of the 4,6-substituted β-D-Glc$p$ residue [3–7]. Therefore, the α-L-Ara$f$-(1 $\rightarrow$ 2)-α-D-Xyl$p$ side chain is attached to the 6-substituted β-D-Glc$p$ residue at the end of the main chain. Thus, the oligoglycosyl alditol in fraction NT-7-5 was assigned the structure SXGol (Fig. 2).

The isomeric oligoglycosyl alditols XSGol and SXGol (fractions NT-7-4 and NT-7-5) differ only in the position of the α-L-Ara$f$ residue. Therefore, comparing the ^{1}H NMR spectra of these two oligoglycosyl alditols reveals correlations between the attachment site of an α-L-Ara$f$-(1 $\rightarrow$ 2)-α-D-Xyl$p$ side chain and the chemical shifts of the α-L-Ara$f$ resonances. For example, the α-L-Ara$f$-(1 $\rightarrow$ 2)-α-D-Xyl$p$ side chain is attached to the 6-substituted β-D-Glc$p$ residue in SXGol, and α-L-Ara$f$ H-1 is observed at δ 5.159. The α-L-Ara$f$-(1 $\rightarrow$ 2)-α-D-Xyl$p$ side chain is attached to the 4,6-substituted β-D-Glc$p$ residue in XSGol, and H-1 of the α-L-Ara$f$ residue is observed at δ 5.172. This important correlation was used as the basis for determining the location of the α-L-Ara$f$-(1 $\rightarrow$ 2)-α-D-Xyl$p$ side chain in several other oligoglycosyl alditols generated from tobacco AXG. Structural assignments made on this basis were confirmed by other techniques (see below), confirming the correlation.

SCSCs diagnostic for the location of the α-L-*Araf*-(1 $\rightarrow$ 2)-α-D-*Xyl*p *side chain.*—A self-consistent set of diagnostic SCSCs became apparent when the complete set of AXG oligoglycosyl alditol resonance assignments (Table 2) was analyzed. For example, α-L-Ara$f$ H-1 is observed at δ 5.159 $\pm$ 0.003 when the α-L-Ara$f$-(1 $\rightarrow$ 2)-α-D-Xyl$p$ side chain is attached to the 6-substituted β-D-Glc$p$ residue at the end of the main chain, and α-L-Ara$f$ H-1 is observed at δ 5.170 $\pm$ 0.003 when this side chain is attached to an internal 4,6-substituted β-D-Glc$p$ residue, as initially observed for the isomers XSGol and SXGol (see above). The α-L-Ara$f$ H-4 resonance is at δ 4.055 $\pm$ 0.004 when the α-L-Ara$f$-(1 $\rightarrow$ 2)-α-D-Xyl$p$ side chain is attached to the 6-substituted Glc$p$ residue, but the α-L-Ara$f$ H-4 resonance is at δ 4.080 $\pm$ 0.002 when this side chain is attached to an internal 4,6-substituted Glc$p$ residue. H-2 of the terminal α-L-Ara$f$ residue is at δ 4.193 $\pm$ 0.002 when the α-L-Ara$f$-(1 $\rightarrow$ 2)-α-D-Xyl$p$ side chain is attached to the 4,6-substituted β-D-Glc$p$ residue linked to the alditol. However, H-2 of the terminal α-L-Ara$f$ residue is at δ 4.200 $\pm$ 0.004 when the side chain is attached to any other β-D-Glc$p$ residue. Thus, the exact position of an α-L-Ara$f$-(1 $\rightarrow$ 2)-α-D-Xyl$p$ side chain in the AXG oligoglycosyl alditols can often be determined by examining the chemical shifts of the H-1, H-2, and H-4 resonances of the α-L-Ara$f$ residue.

SCSCs diagnostic for the branching pattern of the β-D-*Glc*p *residues.*—Oligoglycosyl alditols generated from AXGs have a relatively high proportion of terminal and 4-substituted β-D-Glc$p$ residues (see above). This characteristic makes AXG oligoglycosyl alditols an ideal system for studying the effects of side chain substitution on the chemical shifts of β-D-Glc$p$ resonances. SCSCs diagnostic for various substitution patterns of the β-D-Glc$p$ residues in the backbones of xyloglucan and AXG oligoglycosyl alditols are summarized in Table 4. Generally, the addition of a glycosyl substituent

to a β-D-Glc*p* residue causes a downfield shift of several of its resonances. This allows, for example, terminal β-D-Glc*p* residues to be distinguished from 4-, 6-, and 4,6-substituted β-D-Glc*p* residues. A glycosyl substituent at O-6 of a β-D-Glc*p* residue has small and variable effects on the chemical shifts of H-6 and H-6′, but leads to reproducible downfield shifts for H-5 ($\Delta\delta \sim 0.2$) and H-4 ($\Delta\delta \sim 0.1$). A glycosyl substituent at O-4 causes a downfield shift of H-4 ($\Delta\delta \sim 0.2$) and smaller downfield shifts of H-5 ($\Delta\delta \sim 0.1$) and H-3 ($\Delta\delta \sim 0.1$). More subtle but nevertheless informative chemical-shift effects are observed for H-1 and H-2 of a β-D-Glc*p* residue upon addition of a glycosyl substituent at O-4 and/or O-6.

The H-1 resonance of a β-D-Glc*p* residue linked directly to the glucitol moiety is shifted downfield of other β-D-Glc*p* H-1 resonances [3–7] into a relatively uncluttered region of the spectrum (δ 4.59 → 4.64). The presence of a side chain at O-6 of a β-D-Glc*p* residue linked to the glucitol leads to a small but very reproducible effect on the chemical shift of its H-1 resonance. The chemical shift of this H-1 resonance is greater than δ 4.600 when the β-D-Glc*p* residue bears a side chain at O-6 and less than δ 4.600 when it does not. The chemical shift of this H-1 resonance is less than δ 4.594 when neither of the two β-D-Glc*p* residues closest to the glucitol bears a side chain at O-6. In summary, considerable information regarding the number and location of side chains in the oligoglycosyl alditol can be obtained just by analyzing β-D-Glc*p* H-1 resonances in its 1D ^{1}H NMR spectrum.

Glycosyl-linkage analysis of tobacco AXG.—The glycosyl-linkage compositions (Table 5) of tobacco AXG oligosaccharide fractions NT-3 through NT-8 were determined by methylation analysis. The results are consistent with previous studies [8–10] wherein it was concluded that the backbone of tobacco AXG consists of (1 → 4)-linked Glc*p* residues, approximately 40% of which are substituted at O-6 with Xyl*p* and Ara*f*-(1 → 2)-Xyl*p* side chains. Glycosyl-linkage compositions were also obtained for those highly purified tobacco AXG oligoglycosyl alditols that were available in sufficient quantities for this analysis (Table 5). The structural assignments obtained by NMR spectroscopy of these oligoglycosyl alditols are consistent with their glycosyl-linkage compositions, confirming the SCSCs upon which these structural assignments were based. For example, significant amounts of 2-substituted Xylp residues and terminal Ara*f* residues are components only of those oligoglycosyl alditols whose NMR spectra indicated the presence of an α-Ara*f*-(1 → 2)-α-Xyl*p* side chain. The presence of a terminal Glc*p* residue in fractions NT-3-3-2 (GXSGGol) and LE-4-5 (GXSGol), predicted on the basis of the diagnostic ^{1}H chemical shifts listed in Table 4, is confirmed by these analyses. (Fraction LE-4-5 from tomato AXG was analyzed because it contained a relatively large amount of GXSGol, facilitating its glycosyl-linkage analysis. Smaller amounts of GXSGol were originally detected in fractions NT-5-5 and NT-6-5 from tobacco AXG, see Table 1.) In addition, the presence of at least one unbranched, 4-substituted Glc*p* residue in fractions NT-3-3-1 (XXGGGol), NT-3-3-2 (GXSGGol), NT-3-5 (XSGGGol), NT-4-2 (XSGGol), and NT-6-6-1 (XXGGol), as predicted on the basis of the characteristic upfield shift of H-1 of the β-Glc*p* residue attached to the alditol (see above), is confirmed.

MALDITOFMS of tobacco AXG oligoglycosyl alditols.—The molecular masses of the tobacco AXG oligoglycosyl alditols were measured by MALDITOFMS (Table 1).

Table 4
^{1}H NMR chemical shifts [a] for β-D-Glc*p* residues in the backbone of xyloglucan oligoglycosyl alditols

Linkage Environment	T-Glc*p* End of main chain	6-Glc*p*		4-Glc*p*			4,6-Glc*p*	
		T-α-Xyl*p* side chain	Oligomeric [b] side chain	Between 4,6-Glc*p* and Glcol	Between 4-Glc*p* and Glcol	Between 4,6-Glc*p* and 4-Glc*p*	Linked to Glcol	Not linked to Glcol
δH-1	4.513	4.545	4.530	4.596	4.592	4.544	4.626	4.560
$\sigma(N)$ [c]	0.010	0.009	0.011	0.001	0.001	0.001	0.008	0.017
N [d]	12	14	7	10	5	5	18	32
δH-2	3.320	3.337	3.337	3.388	3.372	3.372	3.417	3.400
$\sigma(N)$ [c]	0.006	0.005	0.006	0.003	0.002	0.002	0.013	0.013
N [d]	12	14	7	9	4	4	17	17
δH-3	3.506	3.521	3.517	3.647	3.642	3.65	3.676	3.669
$\sigma(N)$ [c]	0.002	0.006	0.002	0.002	–	–	0.011	0.011
N [d]	12	12	5	3	1	1	10	11
δH-4	3.414	3.518	3.464	3.688	3.686	3.70	3.683	3.708
$\sigma(N)$ [c]	0.003	0.005	0.003	0.002	–	–	0.074	0.033
N [d]	12	12	6	3	1	1	9	11
δH-5	3.485	3.696	3.744	3.583	3.577	n.a.	3.825	3.844
$\sigma(N)$ [c]	0.005	0.008	–	0.002	–	–	0.053	0.029
N [d]	12	12	1	3	1	–	9	10
δH-6	3.732	3.777	3.813	3.854	3.855	3.82	3.911	3.919
$\sigma(N)$ [c]	0.001	0.010	–	0.001	–	–	0.057	0.028
N [d]	2	12	1	3	1	1	10	11
δH-6′	3.916	3.939	3.883	3.959	3.96	3.97	3.967	3.972
$\sigma(N)$ [c]	0.001	0.003	–	0.001	–	–	0.069	0.044
N [d]	2	12	1	3	1	1	10	11

[a] Data in this table were compiled from chemical-shift measurements described herein and in refs. [3–7], and include data derived from xyloglucans of non-solanaceous plants.

[b] "Oligomeric side chain" indicates that the α-D-Xyl*p* residue linked to O-6 of the Glc*p* residue has a glycosyl substituent at O-2.

[c] $\sigma(N)$ = Root-mean-square deviation.

[d] N = number of Glc*p* residues for which the chemical shift of the proton was measured.

Table 5
Glycosyl-linkage analysis [a] of oligoxyloglucan fractions from tobacco and tomato AXG

Fraction	Structure	Residue and linkage [b]									
		4-Glcol	T-Ara*f*	T-Xyl*p*	T-Glc*p*	3-Ara*f*	T-Gal*p*	2-Xyl*p*	6-Glc*p*	4-Glc*p*	4,6-Glc*p*
NT-3	Mixture [c]	0.0	13.7	14.0	2.9 [d]	0.0	0.0	12.9	8.4	29.2	19.0
NT-4	Mixture [c]	0.0	13.8	14.8	2.1 [d]	0.0	0.0	13.6	11.9	25.4	18.3
NT-5	Mixture [c]	0.0	16.1	16.8	2.3 [d]	0.0	0.0	16.1	12.3	19.9	16.4
NT-6	Mixture [c]	0.0	10.2	19.3	2.3 [d]	0.0	0.0	12.1	14.8	22.5	19.0
NT-7	Mixture [c]	0.0	16.8	16.5	1.5 [d]	0.0	0.0	15.5	16.1	17.6	15.9
NT-8	Mixture [c]	0.0	5.1	26.2	2.9 [d]	0.0	0.0	5.4	20.6	23.8	16.1
NT-3-3-1	XXGGGol	2.1 [d]	0.0	26.9	0.0	0.0	0.0	1.3 [e]	13.4	36.2	17.6
NT-3-3-2	GXSGGol	1.9 [d]	11.5	12.7	7.7 [d]	0.0	0.0	17.2	0.0	16.0	33.0
NT-3-5	XSGGGol	10.2 [d]	15.6	11.1	tr [f]	1.3 [g]	0.0	14.1	11.3	21.4	14.2
NT-4-2	XSGGol	5.5 [d]	16.4	14.8	tr [f]	1.1 [g]	0.0	14.0	14.7	15.1	17.6
NT-6-3	XSGol	3.5 [d]	11.5	16.0	tr [f]	tr [f]	0.0	19.1	21.8	2.0 [h]	25.6
NT-6-6-1	XXGGol	2.6 [d]	0.0	18.8	0.0	0.0	0.0	1.0 [e]	22.7	27.2	26.8
LE-3	Mixture [c]	0.0	6.1	8.5	6.2 [d]	3.1	6.1 [d]	14.7	8.4	23.6	23.2
LE-3-4-2	LXGGol	tr [d,f]	tr [f]	18.1	0.0	0.0	6.7 [d]	14.1	16.0	20.6	24.5
LE-3-4-3	GXTGol	tr [d,f]	6.0	12.8	6.3 [d]	15.3	0.0	11.0	tr [f]	2.7 [h]	45.9
LE-4-5 [i]	GXSGol	6.0 [d]	16.4	17.9	8.3 [d]	tr [f]	tr [f]	19.4	2.3	1.6 [h]	28.2

[a] Normalized mol% of partially methylated alditol acetate derivatives.
[b] Numbers refer to the positions of glycosyl substituents.
[c] Mixture of reducing oligosaccharides.
[d] The derivatives of terminal residues such as T-Glc*p*, T-Gal*p*, and 4-Glcol were usually recovered at lower than expected yields. Needs and Selvendran [38] have investigated the basis for this phenomenon.
[e] Small amounts of the derivative of 2-Xyl*p* in the indicated fractions were attributed to incomplete methylation of T-Xyl*p* residues. The results observed are typical for incomplete methylation of T-Xyl*p* because approximately equimolar amounts of the derivatives of 2-Xyl*p* and 4-Xyl*p* were detected in these fractions. Although these two derivatives cannot be separated by GC, the use of $NaBD_4$ as a reducing agent [20] allowed their detection and quantitation in the indicated fractions (e.g., on the basis of the diagnostic ions at m/z 117 and 118 in their electron impact-mass spectra).
[f] Trace (< 1 mol%) of derivative recovered.
[g] Attributed to incomplete methylation.
[h] Small amounts of the derivative of 4-Glc*p* are generated by oxidation of the glucitol [39] under the conditions used.
[i] Fraction LE-4-5 contained ~ 85% GXSGol.

The results of these analyses were in every case consistent with the structures proposed on the basis of NMR spectroscopy.

FABMS and FABMS / MS of tobacco AXG oligoglycosyl alditols.—Per-*O*-acetylated aliquots of purified tobacco AXG oligoglycosyl alditols were analyzed by FABMS in order to confirm the glycosyl sequence assignments that were based on NMR spectroscopy. FABMS provided accurate molecular mass estimations for the per-*O*-acetylated oligoglycosyl alditols, thereby confirming their glycosyl compositions. The fragmentation patterns observed during FABMS are, in every case, in agreement with the proposed sequences, but in some cases it is difficult to obtain unambiguous sequence information using this technique. Much of the ambiguity is due to the partial cleavage of the labile arabinofuranosyl residues of these oligoglycosyl alditols. Some mass spectra

contained, in addition to the expected quasimolecular $[M + H]^+$ ion, a quasimolecular $[M + H]^+$ ion corresponding in mass to an oligoglycosyl alditol that had lost an Ara*f* residue during the *O*-acetylation reaction. Ions produced by fragmentation of such a partially degraded oligoglycosyl alditol could not be distinguished from "double-cleavage" ions [3,28], produced by secondary decomposition of the intact oligoglycosyl alditol that had survived the *O*-acetylation reaction. However, FABMS/MS allowed the glycosyl sequences of many of the oligoglycosyl alditols to be determined unambiguously.

FABMS/MS spectra of the AXG oligoglycosyl alditols were recorded by collision-activated decomposition (CAD) of their quasimolecular $[M + H]^+$ ions. Unambiguous interpretation of the resulting spectra is usually possible because they consist primarily of high abundance B^+ ions [29,30] derived from the non-reducing end of the oligoglycosyl alditol and lower abundance Z^+ ions [29] derived from the alditol end of the molecule. However, the abundance of $[M + H]^+$ quasimolecular ions generated by FAB ionization of per-*O*-acetylated oligoglycosyl alditols is usually very low compared to that of the quasimolecular $[M + Na]^+$ or $[M + NH_4]^+$ ions. Unfortunately, spectra obtained by CAD of the $[M + Na]^+$ or $[M + NH_4]^+$ ion are complicated and difficult to interpret. Therefore, 18-crown-6 ether was added to the nitrobenzyl alcohol matrix in order to sequester Na^+ and NH_4^+ ions and thereby increase the abundance of the $[M + H]^+$ ions during the FAB ionization process [22]. This technique made it possible to obtain CAD mass spectra that could be readily interpreted in terms of the side chain distribution of the oligoglycosyl alditols.

FABMS/MS facilitates the identification of ions that arise from loss of the labile Ara*f* residues. Parent-ion selection in MS-1 filters out ions arising from partially degraded oligoglycosyl alditols generated by loss of the Ara*f* residue during sample derivatization. Furthermore, secondary fragment ions are more readily identified by FABMS/MS than by FABMS. In general, two ions that differ in mass by 42 amu are formed by secondary fragmentation of a B^+ ion [3,28]. The difference in mass of these two ions arises because the secondary fragmentation can be accompanied by the migration of either a proton or an *O*-acetyl group. Thus, when a pair of ions separated by 42 amu is encountered, these ions can often be identified as "double-cleavage" ions [3,28]. However, it is also possible for a primary B^+ ion formed during FAB ionization to simply lose an *O*-acetyl substituent, leading to the formation of an ion that is separated from the primary B^+ ion by 42 amu. Thus, it is sometimes difficult to distinguish primary B^+ ions from "double-cleavage" ions detected during FABMS of per-*O*-acetylated oligoglycosyl alditols. In contrast, *O*-acetyl substituents are rarely lost by B^+ ions observed during FABMS/MS of these molecules [30], allowing pairs of ions separated by 42 amu in the resulting spectra to be reliably identified as "double-cleavage" ions.

The location of the α-Ara*f*-(1 → 2)-α-Xyl*p* side chains in the isomers XSGol and SXGol are confirmed by analysis of the FABMS/MS spectra of their per-*O*-acetylated derivatives (Fig. 4). The side chain that is attached to Glc^b (i.e., the β-Glc*p* residue at the non-reducing end of the main chain of each of these two oligoglycosyl alditols) was identified by comparing the mass of B^+ ions formed by fragmentation of the glycosidic bond of Glc^b. The B^+ ion at m/z 547 (XylGlc) indicates that a monopentosyl side

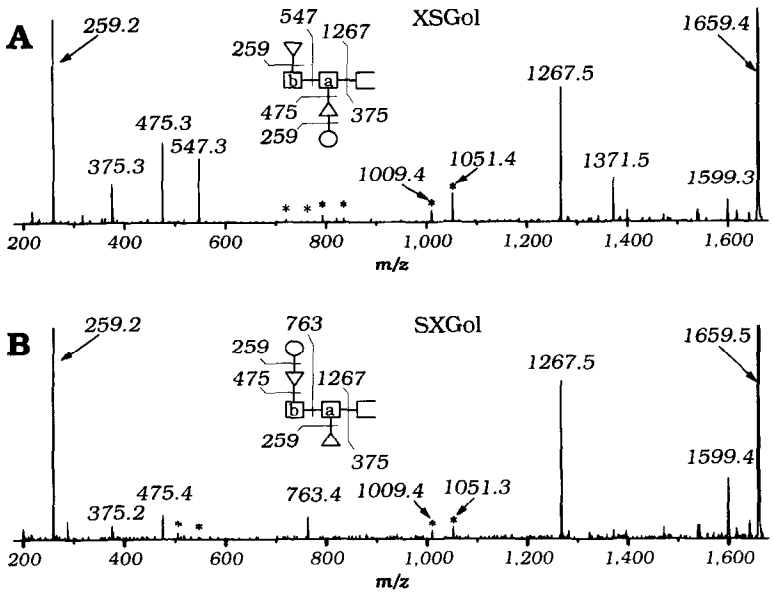

Fig. 4. FABMS/MS of the per-*O*-acetylated derivatives of the tobacco AXG oligoglycosyl alditols XSGol (A) and SXGol (B). Collision-activated decomposition (CAD) fragments of the quasimolecular $[M+H]^+$ ions were analyzed in MS-2. Calculated nominal masses are indicated in the fragmentation diagram, and measured monoisotopic masses are indicated for the ions observed in the spectra. Double-cleavage ions [3,28] at *m/z* 721, 763, 793, 835, 1009, and 1051 in the spectrum of XSGol and at *m/z* 505, 547, 1009, and 1051 in the spectrum of SXGol are indicated by asterisks.

chain is attached to Glc^b of XSGol and the B^+ ion at *m/z* 763 (AraXylGlc) indicates that a dipentosyl side chain is attached to Glc^b of SXGol. Low-abundance ions at *m/z* 763 in the spectrum of XSGol and at *m/z* 547 in the spectrum of SXGol were readily identified as "double-cleavage" ions (see above) by virtue of the high abundance of the related ions having 42 amu less mass (i.e., *m/z* 721 and *m/z* 505, respectively). The ions at *m/z* 1,051 (Xyl_2Glc_2 or $AraXylGlc_2$) in both spectra were also identified as double-cleavage ions because of the high abundance of the ions at *m/z* 1,009. Thus, the FABMS/MS spectra (Fig. 4) of these oligoglycosyl alditols are consistent with the structures proposed on the basis of their NMR spectra (see above).

Glycosyl sequences of 14 of the AXG oligoglycosyl alditols were unambiguously deduced by FABMS (XSGGol, XXGGGol, GXSGGol, GSSGGol, XSGGGol, GSGGol, XGGGol, and XXGGol) and FABMS/MS (XSGol, SXGol, SGGGol, GXSGol, GSGol, and SGGol). FABMS/MS spectra of many of the oligoglycosyl alditols could not be obtained, due to lack of sufficient material or to instrumental (mass-range) limitations. In some cases, FABMS alone was not sufficient to obtain an unambiguous sequence, due to the experimental difficulties outlined above. However, those sequences (listed above) that could be unambiguously deduced by MS are consistent with the structural assignments obtained by NMR spectroscopy. These results indicate that the SCSCs deduced by examination of the full set of NMR spectra are not only self-consistent, but

are accurate reflections of the chemical structures of these oligoglycosyl alditols, and can therefore be used as diagnostic tools for the structural identification of these molecules.

Analysis of tomato AXG.—The ^{1}H NMR spectra of the Bio-Gel P-2 fractions LE-3 through LE-7 (Fig. 1B) derived from tomato AXG included several resolved resonances that were not observed in the ^{1}H NMR spectra of the oligoglycosyl alditols from tobacco AXG. Cross-peaks in the COSY and TOCSY spectra of fraction LE-4 suggested that the additional resonances were due to a non-reducing terminal β-D-Gal*p* residue and an unknown component that had not previously been observed in xyloglucans. Fractions LE-3 and LE-4 were therefore reduced to the corresponding oligoglycosyl alditols and further purified by reversed-phase HPLC. The resulting chromatograms (not shown) are at least as complex as those obtained during reversed-phase chromatography of the tobacco AXG oligoglycosyl alditols, described above and in Table 1. Furthermore, ^{1}H NMR analysis showed that, although most of the HPLC fractions derived from fractions NT-3 and NT-4 contained a single oligoglycosyl alditol, each HPLC fraction derived from fractions LE-3 and LE-4 contained at least two oligoglycosyl alditols. Thus, fractions LE-3 and LE-4 from tomato AXG are significantly more heterogeneous than fractions NT-3 and NT-4 from tobacco AXG. Emphasis was placed on the purification of oligoglycosyl alditols representing the novel structural features of tomato AXG. Two such oligoglycosyl alditols (LXGGol and GXTGol, Fig. 1) were further purified by HPAEC of fraction LE-3-4 and structurally characterized.

NMR analysis of fraction LE-3-4-2.—The ^{1}H NMR spectrum of fraction LE-3-4-2 (Fig. 3C) indicates that its main component (~ 80% of the fraction) is a hexaglycosyl alditol. Each (major) anomeric resonance of LE-3-4-2 was assigned to a specific isolated spin system by analyzing the COSY and TOCSY spectra of this fraction. The stereochemistry and chemical environment of each spin system was assigned (Table 2) by comparing the chemical shifts and coupling constants of its resonances to those of previously described oligoglycosyl alditols [3–7]. Thus, the signal at δ 5.158 ($^3J_{1,2}$ 3.6 Hz) was assigned as H-1 of an α-D-Xyl*p* residue with a β-D-Gal*p* substituent at O-2, and the resonance at δ 4.562 ($^3J_{1,2}$ 7.8 Hz) was assigned as H-1 of a terminal β-D-Gal*p* residue attached to O-2 of an α-D-Xyl*p* residue. The resonance at δ 4.957 was assigned as H-1 of a terminal α-D-Xyl*p* residue attached to O-6 of a 4,6-substituted β-D-Glc*p* residue (see the above discussion of XSGol and SXGol). The resonance at δ 4.596 ($^3J_{1,2}$ 8 Hz) was assigned as H-1 of β-D-Glc*p* residue attached to the glucitol moiety. The chemical shift of this resonance indicates that this β-D-Glc*p* residue does not bear a side chain at O-6 (see above and Table 4). The resonances at δ 4.572 and δ 4.544 were assigned as H-1 of a 4,6-substituted β-D-Glc*p* (not linked directly to the glucitol) and a 6-substituted β-D-Glc*p* residue, respectively (see Table 4). Taken together, these assignments indicate that fraction LE-3-4-2 contains LXGGol as its most abundant component. This structural assignment is supported by the results of other analytical techniques (see below).

NMR analysis of fraction LE-3-4-3.—The ^{1}H NMR spectrum of fraction LE-3-4-3 (Fig. 3D) indicates that it contains a homogeneous heptaglycosyl alditol. Most of the anomeric resonances of LE-3-4-3 and the spin systems to which they belong (Table 2) were assigned by analysis of the COSY and TOCSY spectra of this fraction. The

resonance at δ 5.088 ($^3J_{1,2}$ 3.6 Hz) was assigned as H-1 of an α-D-Xyl*p* residue having an α-L-Ara*f* substituent at O-2 [3,8], and the resonance at δ 4.957 ($^3J_{1,2}$ 3.6 Hz) was assigned as H-1 of a terminal α-D-Xyl*p* residue that is linked to O-6 of a 4,6-substituted β-D-Glc*p* residue [3–7]. Spin systems corresponding to a 4,6-substituted β-D-Glc*p* residue that is attached directly to the alditol (β-Glc^a, H-1 δ 4.638, $^3J_{1,2}$ 8 Hz), a 4,6-substituted β-D-Glc*p* residue that is not attached directly to the alditol (β-Glc^b, H-1 δ 4.547, $^3J_{1,2}$ 8 Hz), and a non-reducing terminal β-D-Glc*p* residue (β-Glc^c, H-1 δ 4.519, $^3J_{1,2}$ 8 Hz) were also assigned [3–7]. In addition, the resonances at δ 5.089 (H-1), δ 4.159 (H-2), and δ 4.097 (H-3) are part of an isolated spin system having the characteristic scalar-coupling pattern of a β-Ara*f* residue (Table 3). The resonance at δ 5.175 ($^3J_{1,2}$ 1.8 Hz) was assigned as H-1 of an α-L-Ara*f* residue [3–8] (Tables 1 and 3). However, all of the protons of this α-L-Ara*f* residue are deshielded compared to those of the non-reducing terminal α-L-Ara*f* residues in the oligoglycosyl alditols isolated from tobacco AXGs (see Table 2), suggesting that the α-L-Ara*f* residue in fraction LE-3-4-3 bears a glycosyl substituent.

The identity and location of the glycosyl substituent of the α-L-Ara*f* residue in fraction LE-3-4-3 were determined by analysis its ROESY spectrum. Analysis of this spectrum is complicated by the overlap of the H-1 resonances of the β-Ara*f* and the 2-substituted α-D-Xyl*p* residues (δ 5.09, Fig. 3D and Table 2). Nevertheless, a strong cross-peak (δ_1 5.09, δ_2 3.975) in the ROESY spectrum was attributed to the interaction of H-1 of the β-Ara*f* residue with H-3 of the α-L-Ara*f* residue, indicating that the β-Ara*f* residue is glycosidically linked to O-3 of the α-L-Ara*f* residue. Another cross-peak (δ_1 5.09, δ_2 3.890) was attributed to the interaction of H-1 of the 2-substituted α-D-Xyl*p* residue with H-6 of β-Glc^a. Although it is possible that the interaction of H-1 of the 2-substituted α-D-Xyl*p* residue with H-6′ of β-Glc^a (δ 3.974) contributes to the cross-peak at δ_1 5.09, δ_2 3.98, the shape of this cross-peak (in the F_2 dimension) suggests that it arises primarily from the interaction of β-Ara*f* H-1 with α-Ara*f* H-3. In addition, the ROESY spectrum contains a strong cross-peak (δ_1 5.18, δ_2 3.57) arising from the interaction of H-1 of the α-L-Ara*f* residue with H-2 of the 2-substituted α-D-Xyl*p* residue. Taken together, the ROESY data for LE-3-4-3 is consistent with the presence of a β-Ara*f*-(1 → 3)-α-L-Ara*f*-(1 → 2)-α-D-Xyl*p* side chain at O-6 of the β-D-Glc*p* residue linked to the alditol. This structure has not been previously reported as a side chain in a xyloglucan, and we have assigned the one-letter code [31] T (mnemonic, Tomato) for a β-D-Glc*p* residue bearing this side chain at O-6. The structure GXTGol (Fig. 2), based on the complete set of 2D NMR data for fraction LE-3-4-3, was confirmed by other techniques (see below).

Glycosyl-linkage analysis of tomato AXG oligoglycosyl alditols.—Glycosyl-linkage analysis of the oligosaccharides generated by EG-digestion of tomato AXG (e.g., fraction LE-3, Table 5) revealed the presence of 3-substituted Ara*f* and terminal Gal*p* residues that were not present in the tobacco AXG oligosaccharides (fractions NT-3 through NT-8, Table 5). The glycosyl-linkage compositions of the highly purified oligoglycosyl alditols in fractions LE-3-4-2 and LE-3-4-3 (Table 5) are in qualitative agreement with the structures proposed on the basis of NMR analysis. For example, this analysis confirmed that the unbranched Glc*p* residue in fraction LE-3-4-2 (LXGGol) is 4-substituted, and the unbranched Glc*p* residue in fraction LE-3-4-3 (GXTGol) is

terminal. The detection of terminal Gal*p* and 2-substituted Xyl*p* residues in fraction LE-3-4-2 confirm the structure of the β-D-Gal*p*-(1 → 2-)α-D-Xyl*p* side chain of LXGGol. The detection of terminal Ara*f*, 3-substituted Ara*f*, and 2-substituted Xyl*p* residues in LE-3-4-3 confirm the structure of the β-L-Ara*f*-(1 → 3)-α-L-Ara*f*-(1 → 2)-α-D-Xyl*p* side chain of GXTGol, proposed on the basis of cross peaks in the ROESY spectrum of LE-3-4-3 (see above).

Mass spectrometry of tomato AXG oligoglycosyl alditols.—Quasimolecular $[M + Na]^+$ ions in the MALDITOF mass spectra of the oligoglycosyl alditol fractions LE-3-4-2 and LE-3-4-3 from tomato AXG are consistent with the structures proposed on the basis of the NMR spectroscopy, i.e., LXGGol (measured $m/z = 1118.1$, calculated $m/z = 1118.0$) and GXTGol (measured $m/z = 1218.9$, calculated $m/z = 1220.1$).

The FAB mass spectra of the per-*O*-acetylated derivatives of these oligoglycosyl alditols were also consistent with these structures. Several diagnostic fragment ions are present in the FAB mass spectrum of LE-3-4-2. For example, B^+ ions formed by cleavage of the glucan backbone of the oligoglycosyl alditol correspond in mass to GalXylGlc (m/z 835), $GalXyl_2Glc_2$ (m/z 1,339), and $GalXyl_2Glc_3$ (m/z 1,627), and indicate that the β-D-Gal*p*-(1 → 2)-α-D-Xyl*p* side chain is attached to Glc^c and a α-D-Xyl*p* side chain is attached to Glc^b. This spectrum also contains a strong Z^+ ion at m/z 663 (GlcGlcol), indicating that the Glc*p* residue attached to the alditol is not branched. It should be noted that a contaminant of unknown origin sometimes gives rise to an ion at m/z 663 in the FAB mass spectra of per-*O*-acetylated oligoglycosyl alditols. However, the contaminant ion is unusual in that isotopomers at m/z 661, 662, 663, and 664 are detected in the ratio 0.25:0.7:1.0:0.4, suggesting that its elemental components are not limited to C, H, and O. Conversely, the isotopomer abundance for the Z^+ fragment ion (GlcGlcol) over this range is 0.0:0.0:1.0:0.33, allowing it to be readily distinguished from the contaminant. Thus, the m/z 663 ion in the FAB mass spectrum of LE-3-4-2 was identified as a Z^+ ion (GlcGlcol) by its isotopomer distribution, providing additional evidence in support of the structure (LXGGol) proposed for the main component of this fraction.

The FABMS of per-*O*-acetylated NT-3-4-3 (Fig. 5) is consistent with the structure GXTGol. The series of B^+ ions at m/z 259 (Ara), m/z 475 (Ara_2), and m/z 691 (Ara_2Xyl) arise from the novel β-Ara*f*-(1 → 3)-α-L-Ara*f*-(1 → 2)-α-D-Xyl*p* side chain. The Z^+ ion at m/z 1,311 indicates that this tripentosyl side chain is attached to Glc^a. Fragmentation of the glucan backbone produces the series of B^+ ions at m/z 331 (Glc), m/z 835 ($XylGlc_2$), and m/z 1,771 ($Ara_2Xyl_2Glc_3$), further supporting the proposed locations of the side chains of this oligoglycosyl alditol.

The presence of a β-Ara*f* residue in GXTGol produces some noteworthy features in the FAB mass spectra of its per-*O*-acetylated derivative (Fig. 5). The B^+ ions at m/z 1,771 and m/z 691 in this spectrum, both of which contain the novel β-Ara*f*-(1 → 3)-α-L-Ara*f*-(1 → 2)-α-D-Xyl*p* side chain, appear to readily lose acetic acid (60 amu) by an elimination reaction, forming ions at m/z 1711 and m/z 631, respectively. The m/z 631 ion then appears to lose an additional 102 amu by elimination of acetic anhydride, forming the ion at m/z 529. The ion at m/z 1753 corresponds to $[M + Na]^+$ for per-*O*-acetylated Xyl_2Glc_3Glcol, and probably is due to loss of the two labile Ara*f* residues during the acid-catalyzed acetylation reaction. The B^+ ion at m/z 1339

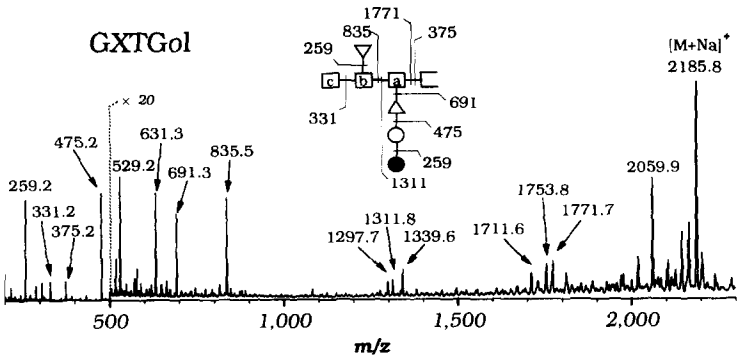

Fig. 5. FAB mass spectrum of the per-*O*-acetylated derivative of GXTGol. Calculated nominal masses are indicated in the fragmentation diagram, and measured monoisotopic masses are indicated for the ions observed in the spectrum. The ions at *m/z* 1297, 1339, and 1753 are due to cleavage of the labile Ara*f* residues of GXTGol (see text).

(Xyl_2Glc_3) may arise by fragmentation of Xyl_2Glc_3Glcol and/or by double-cleavage in the FAB source (i.e., loss of Ara_2 from the *m/z* 1,771 B^+ ion). This interpretation is consistent with the presence of a high-abundance ion (*m/z* 1297) having 42 amu less mass (see above).

Side chain distribution and biological function in AXGs.—The branched structure of xyloglucans undoubtedly gives rise to many of the unique physical properties that are required for the proper functionality of these polysaccharides in vivo. A regular branching pattern is well documented [1] for the fucose-containing xyloglucans produced by non-solanaceous plants. Typically every fourth β-D-Glc*p* residue in this type of xyloglucan is unbranched, and almost all of the fucose-containing side chains are linked to O-6 of β-D-Glc*p* residues that are linked to O-4 of these unbranched β-D-Glc*p* residues. This arrangement restricts the distance between β-D-Glc*p* residues bearing fucose-containing side chains to a multiple of four residues.

The regular branching pattern of xyloglucans probably leads to molecular topologies that facilitate their binding to cellulose [1,32]. It is likely that, upon binding to cellulose, the backbone of a xyloglucan adopts a flat, ribbon-like structure wherein the alternating orientation of the β-D-Glc*p* residues places side chains on alternating edges of the backbone [32]. The regular distribution pattern of fucose-containing side chains (see above), combined with the hypothetical tendency for all of these side chains to adopt similar conformations, may cause a series of these fucose-containing side chains to fold onto one face of the xyloglucan backbone [32]. The α-(1 → 6) glycosidic linkages of the monoxylosyl side chains are likely to be very flexible, allowing the terminal α-Xyl*p* residues to fold onto the same face of the xyloglucan as do the fucose-containing side chains, thus freeing one of the faces of the xyloglucan backbone for binding to a cellulose microfibril.

Structural analysis of the oligosaccharides generated by EG-treatment of endogenously *O*-acetylated tobacco AXG suggests that long stretches of unbranched β-D-Glc*p* residues are not present in the backbone of this polymer. The "average" oligosaccharide

generated by EG-treatment of tobacco AXG has approximately four β-D-Glc*p* residues in its backbone, and 41% of these β-D-Glc*p* residues are branched. This is in good agreement with the amount of branching (40–45%) obtained by analysis of intact tobacco AXG. This suggests that nearly all of the unbranched β-D-Glc*p* residues in tobacco AXG are located within three residues of a branched β-D-Glc*p* residue, and is consistent with a more or less regular distribution of branched residues in the AXG.

The *O*-acetyl substituents attached to O-6 of the β-D-Glc*p* residues of the tobacco AXG backbone may play a role in maintaining a regular side chain distribution during the biosynthesis of the AXG. For example, recognition of glycosyl side chains may direct the *O*-acetyl transferase to specific *O*-acetyl acceptor sites on the AXG, and recognition of *O*-acetyl substituents may direct the xylosyl and/or arabinosyl transferases to specific glycosyl acceptor sites on the AXG, leading to a regular substitution pattern. The *O*-acetyl substituents may also stabilize molecular conformations that either help to maintain AXG solubility in the absence of cellulose or facilitate the binding of AXG to cellulose when it is present.

The α-L-Ara*f*-(1 → 2)-α-D-Xyl*p* side chains of tobacco AXG may have a tendency to fold onto one face of the AXG as it binds to a cellulose microfibril. This type of folding would be favored if the diglycosyl side chains are regularly spaced (e.g., on every fourth or eighth β-D-Glc*p* residue) and all tend to adopt a very similar conformation. The structural features of tobacco AXG, described herein, are consistent with the existence of structural domains in which the diglycosyl (arabinose-containing) side chains have such a regular spacing pattern. However, analysis of larger oligosaccharide fragments of the AXG will be necessary in order to establish whether such regular domains exist.

The 2,4-D stimulated elongation of etiolated pea-stems is inhibited by xyloglucan oligosaccharides with fucose-containing side chains [33,34]. These xyloglucan oligosaccharides are released by endolytic enzymes that are active during the auxin-stimulated expansion of the primary cell wall [35]. Therefore, it has been suggested that fucose-containing oligosaccharides are signaling molecules that regulate elongation of the primary cell wall during growth [33,35]. However, no fucosyl residues have been found in the AXGs produced by solanaceous plants. It is possible that solanaceous plants have acquired mechanisms for maintaining tight control over cell-wall elongation that do not depend on recognition of xyloglucan oligosaccharides. However, one could also speculate that arabinose-containing xyloglucan oligosaccharides act as growth regulators in solanaceous plants, playing a role similar to that proposed for fucose-containing xyloglucan oligosaccharides in other plants.

4. Conclusions

Diagnostic structure–chemical-shift correlations (SCSCs) were observed in the NMR spectra of 20 oligoglycosyl alditols that were generated by reduction of EG-treated tobacco AXG and purified by liquid chromatography. Application of these SCSCs to the NMR data provides a self-consistent set of structural assignments. More importantly, these structural assignments are consistent with data obtained by several independent

spectroscopic and chemical methods. These analyses revealed significant structural homology between the AXGs produced by two evolutionarily related plant species, tobacco and tomato. However, at least two side chain structures, β-D-Gal*p*-(1 → 2)-α-D-Xyl*p* and β-Ara*f*-(1 → 3)-α-L-Ara*f*-(1 → 2)-α-D-Xyl*p*, are present in tomato AXG but not in tobacco AXG. The structures obtained by these analyses suggest, but do not prove, that α-L-Ara*f*-(1 → 2)-α-D-Xyl*p* side chains may be regularly spaced along the tobacco AXG backbone. Such a regular spacing of arabinose-containing side chains would support the hypothesis that the xyloglucans of non-solanaceous plants and the AXGs of solanaceous plants have similar functions in the primary cell wall.

Acknowledgements

This research is supported by United States Department of Energy (DOE) grant DE-FG05-93ER20015, and by the DOE-funded (DE-FG05-93ER20097) Center for Plant and Microbial Complex Carbohydrates. The authors thank Dr. Marcia Kieliszewski and Stefan Eberhard for providing the tomato and tobacco cell culture filtrates, Karen Howard for assistance with the preparation of this manuscript, Lisa K. Harvey for technical assistance, Dr. John Glushka for helpful discussions, and Dennis Warrenfeltz for technical support and maintenance of the NMR and mass spectrometers.

References

[1] T. Hayashi, *Annu. Rev. Plant Physiol. Plant Mol. Biol.*, 40 (1989) 139–168.
[2] P. Kooiman, *Rec. Trav. Chim.*, 80 (1961) 849–865.
[3] W.S. York, H. van Halbeek, A.G. Darvill, and P. Albersheim, *Carbohydr. Res.*, 200 (1990) 9–31.
[4] L.L. Kiefer, W.S. York, P. Albersheim, and A.G. Darvill, *Carbohydr. Res.*, 197 (1990) 139–158.
[5] M. Hisamatsu, W.S. York, A.G. Darvill, and P. Albersheim, *Carbohydr. Res.*, 227 (1992) 45–71.
[6] W.S. York, L.K. Harvey, R. Guillen, P. Albersheim, and A.G. Darvill, *Carbohydr. Res.*, 248 (1993) 285–301.
[7] W.S. York, G. Impallomeni, M. Hisamatsu, P. Albersheim, and A.G. Darvill, *Carbohydr. Res.*, 267 (1995) 79–104.
[8] M. Mori, S. Eda, and K. Kato, *Carbohydr. Res.*, 84 (1980) 125–135.
[9] S. Eda, H. Kodama, Y. Akiyama, M. Mori, K. Kato, A. Ishizu, and J. Nakano, *Agric. Biol. Chem.*, 47 (1983) 1791–1797.
[10] Y. Akiyama and K. Kato, *Phytochemistry*, 21 (1982) 2112–2114.
[11] S.G. Ring and R.R. Selvendran, *Phytochemistry*, 20(11) (1981) 2511–2519.
[12] W. Klop and P. Kooiman, *Biochim. Biophys. Acta*, 99 (1965) 102–120.
[13] J.S.G. Reid, M. Edwards, and I.C.M. Dea, in G.O. Phillips, P.A. Williams, and D.J. Wedlock (Eds.), *Gums and Stabilizers for the Food Industry 4*, IRL Press, Oxford, 1988, pp 391–398.
[14] E.M. Linsmaier and F. Skoog, *Physiol. Plant.*, 18 (1965) 100–127.
[15] J.J. Smith, E.P. Muldoon, and D.T.A. Lamport, *Phytochemistry*, 23 (1984) 1233–1239.
[16] F.M. DuPont, L.C. Staraci, B. Chou, B.R. Thomas, B.G. Williams, and J.B. Mudd, *Plant Physiol.*, 77 (1985) 64–68.
[17] Z. Dische, *Methods Carbohydr. Chem.*, 1 (1962) 478–481.
[18] I. Ciucanu and F. Kerek, *Carbohydr. Res.*, 131 (1984) 209–217.
[19] K.R. Anumula and P.B. Taylor, *Anal. Biochem.*, 203 (1992) 101–108.
[20] W.S. York, A.G. Darvill, M. McNeil, T.T. Stevenson, and P. Albersheim, *Methods Enzymol.*, 118 (1985) 3–40.

[21] A. Dell and P.R. Tiller, *Biochem. Biophys. Res. Commun.*, 3 (1986) 1126–1134.
[22] R. Orlando, *Anal. Chem.*, 64 (1992) 332–334.
[23] M. Rance, O.W. Sorensen, G. Bodenhausen, G. Wagner, R.R. Ernst, and K. Wüthrich, *Biochem. Biophys. Res. Commun.*, 117 (1983) 479–485.
[24] A. Bax and D.G. Davis, *J. Magn. Reson.*, 65 (1985) 355–360.
[25] M. Rance, *J. Magn. Reson.*, 74 (1987) 557–564.
[26] D. Marion and K. Wüthrich, *Biochem. Biophys. Res. Commun.*, 113 (1983) 967–974.
[27] W.S. York, J.E. Oates, H. van Halbeek, A.G. Darvill, and P. Albersheim, *Carbohydr. Res.*, 173 (1988) 113–132.
[28] A. Dell, *Adv. Carbohydr. Chem. Biochem.*, 45 (1987) 19–72.
[29] C.E. Costello and J.E. Vath, *Methods Enzymol.*, 193 (1990) 738–768.
[30] B. Domon, D.R. Müller, and W.J. Richter, *Biomed. Mass Spectrom.*, 19 (1995) 390–392.
[31] S.C. Fry, W.S. York, P. Albersheim, A.G. Darvill, T. Hayashi, J.-P. Joseleau, Y. Kato, E.P. Lorences, G.A. Maclachlan, M. McNeil, A.J. Mort, J.S.G. Reid, H.U. Seitz, R.R. Selvendran, A.G.J. Voragen, and A.R. White, *Physiol. Plant.*, 89 (1993) 1–3.
[32] S. Levy, W.S. York, R. Stuike-Prill, B. Meyer, and L.A. Staehelin, *Plant J. Cell Mol. Biol.*, 1(2) (1991) 195–215.
[33] W.S. York, A.G. Darvill, and P. Albersheim, *Plant Physiol.*, 75 (1984) 295–297.
[34] G.J. McDougall and S.C. Fry, *Plant Physiol.*, 89 (1989) 883–887.
[35] G.J. McDougall and S.C. Fry, *J. Plant Physiol.*, 137 (1991) 332–336.
[36] Y. Akiyama, M. Mori, and K. Kato, *Agric. Biol. Chem.*, 44 (1980) 2487–2489.
[37] D.T.A. Lamport, *Methods Enzymol.*, 106 (1984) 523–528.
[38] P.W. Needs and R.R. Selvendran, *Carbohydr. Res.*, 254 (1994) 229–244.
[39] W.S. York, L.L. Kiefer, P. Albersheim, and A.G. Darvill, *Carbohydr. Res.*, 208 (1990) 175–182.